prions (Fig. 3c). Meanwhile, when inoculated with sCJD-VV2 prions, the 129M/M mice and the 129V/V mice showed a few plaque-type deposits besides synaptic-type deposition in the grey matter. The pattern of PrP deposition in the129M/M mice inoculated with sCJD-VV2 prions was similar to that of the 129M/M mice inoculated with p-dCJD prions.

Western blot analysis revealed that the size of PrP^{res} in the brains was maintained after cross-sequence transmission of sCJD-MM1 prions but not sCJD-VV2 prions (Fig. 3d). The 129V/V mice inoculated with sCJD-MM1 prions produced type 1 PrP^{res}, which were identical in size to those from the 129M/M mice. However, the 129M/M mice inoculated with sCJD-VV2 prions produced the intermediate type PrP^{res} with an upward size shift from the inoculated type 2 template. Thus, the 129M/M mice inoculated with sCJD-VV2 prions showed the prolonged incubation time, plaque-type PrP deposition, and the accumulation of the intermediate type PrP^{res} in the brain. These results suggest that p-dCJD could be caused by cross-sequence transmission of sCJD-VV2 prions to individuals with the 129M/M genotype. The long incubation time of the 129M/M mice inoculated with sCJD-VV2 prions may indicate the frightening possibility that the numbers of p-dCJD patients could increase in the future.

To date, some similarities among sCJD-VV2, p-dCJD and sCJD cases with the 129M/V genotype and type 2 PrP^{Sc} (sCJD-MV2) have been described.[6,13–16] Since sCJD-MV2 account for 11% of German sCJD patients,[26] further transmission studies are needed to elucidate whether sCJD-MV2 prions can cause p-dCJD.

INSTRUCTIONS FOR TRACEBACK STUDY

To compare precisely the susceptibility of the experimental animals with different PrP genotypes in a traceback study, knock-in mice have an advantage over transgenic mice because they have the identical genetic background and the identical PrP expression level.[21] The expression level of PrP affects the length of the incubation period regardless of the PrP genotype. Fortunately, the Tg+Ki-Hu129M_{4R}/M_{4R} mice used in this study were less susceptible to p-dCJD prions than Ki-Hu129V/V mice despite their high expression level of human PrP. However, the Tg+Ki-Hu129M_{4R}/M_{4R} mice showed ~100 days shorter incubation period than the Ki-Hu129M/M mice. Therefore, a traceback study should be performed with knock-in mice but not transgenic mice.

It is unclear whether the emerging prion strain retains the ability for traceback after serial passages in the new host. This question is important in cases in which the emerging prion strain is transmitted horizontally in a new host. Two passages of a mouse scrapie strain 139A in hamsters generated a variant strain that had twice the incubation period of 139A in mice.[27] If the adaptation to the new host PrP is accomplished during passages, the memory of the parental prions may disappear. To elucidate whether the memory of the parental prions and the ability for traceback can be retained over serial passages, further transmission studies are needed.

CONCLUSION

These findings demonstrate that traceback studies can be powerful tools to identify the origin of prions when atypical prion strains emerge through cross-sequence transmission.

ACKNOWLEDGMENTS

We thank H. Kudo and K. Abe for technical assistance, and B. Bell for critical review of the manuscript. This study was supported by the Program for Promotion of Fundamental Studies in Health Sciences of National Institute of Biomedical Innovation (S.M. and T.K.), a grant from the Ministry of Health, Labor and Welfare (A.K., S.M. and T.K.), and a Grant-in-Aid for Scientific Research from the Ministry of Education, Culture, Sports, Science and Technology (A.K. and T.K.).

REFERENCES

1. Prusiner SB, Scott MR, DeArmond JP, Cohen FE. Prion protein biology. *Cell* 1998; **93**: 337–348.
2. Korth C, Kaneko K, Groth D *et al.* Abbreviated incubation times for human prions in mice expressing a chimeric mouse-human prion protein transgene. *Proc Natl Acad Sci USA* 2003; **100**: 4784–4789.
3. Scott M, Foster D, Mirenda C *et al.* Transgenic mice expressing hamster prion protein produce species-specific scrapie infectivity and amyloid plaques. *Cell* 1989; **59**: 847–857.
4. Prusiner SB, Scott M, Foster D *et al.* Transgenic studies implicate interactions between homologous PrP isoforms in scrapie prion replication. *Cell* 1990; **63**: 673–686.
5. Parchi P, Castellani R, Capellari S *et al.* Molecular basis of phenotypic variability in sporadic Creutzfeldt-Jakob disease. *Ann Neurol* 1996; **39**: 767–778.
6. Parchi P, Giese A, Capellari S *et al.* Classification of sporadic Creutzfeldt-Jakob disease based on molecular and phenotypic analysis of 300 subjects. *Ann Neurol* 1999; **46**: 224–233.
7. Parchi P, Capellari S, Chen SG *et al.* Typing prion isoforms. *Nature* 1997; **386**: 232–234.

© 2009 Japanese Society of Neuropathology

8. Parchi P, Zou W, Wang W *et al.* Proc Natl Acad. *Sci USA* 2000; **97**: 10168–10172.
9. Doh-ura K, Kitamoto T, Sakaki Y, Tateishi J. CJD discrepancy. *Nature* 1991; **353**: 801–802.
10. Brown P, Preece M, Brandel JP *et al.* Iatrogenic Creutzfeldt-Jakob disease at the millennium. *Neurology* 2000; **55**: 1075–1081.
11. Hoshi K, Yoshino H, Urata J, Nakamura Y, Yanagawa H, Sato T. Creutzfeldt-Jakob disease associated with cadaveric dura mater grafts in Japan. *Neurology* 2000; **55**: 718–721.
12. Nakamura Y, Watanabe M, Nagoshi K *et al.* Update: Creutzfeldt-Jakob disease associated with cadaveric dura mater grafts-Japan, 1979–2003. *MMWR Morb Mortal Wkly Rep* 2003; **52**: 1179–1181.
13. Shimizu S, Hoshi K, Muramoto T *et al.* Creutzfeldt-Jakob disease with florid-type plaques after cadaveric dura mater grafting. *Arch Neurol* 1991; **56**: 357–362.
14. Mochizuki Y, Mizutani T, Tajiri N *et al.* Creutzfeldt-Jakob disease with florid plaques after cadaveric dura mater graft. *Neuropathology* 2003; **23**: 136–140.
15. Kretzschmar HA, Sethi S, Földvári Z *et al.* Iatrogenic Creutzfeldt-Jakob disease with florid plaques. *Brain Pathol* 2003; **13**: 245–249.
16. Satoh K, Muramoto T, Tanaka T *et al.* Association of an 11–12 kDa protease-resistant prion protein fragment with subtypes of dura graft-associated Creutzfeldt-Jakob disease and other prion diseases. *J Gen Virol* 2003; **84**: 2885–2893.
17. Noguchi-Shinohara M, Hamaguchi T, Kitamoto T *et al.* Clinical features and diagnosis of dura mater graft-associated Creutzfeldt-Jakob disease. *Neurology* 2007; **69**: 360–367.
18. Lane KL, Brown P, Howell DN *et al.* Creutzfeldt-Jakob disease in a pregnant woman with an implanted dura mater graft. *Neurosurgery* 1994; **34**: 737–740.
19. Kopp N, Streichenberger N, Deslys JP, Laplanche JL, Chazot G. Creutzfeldt-Jakob disease in a 52-year-old woman with florid plaques. *Lancet* 1996; **348**: 1239–1240.
20. Takashima S, Tateishi J, Taguchi Y, Inoue H. Creutzfeldt-Jakob disease with florid plaques after cadaveric dural graft in a Japanese woman. *Lancet* 1997; **350**: 865–866.
21. Kimura K, Nonaka A, Tashiro H *et al.* Atypical form of dura graft associated Creutzfeldt-Jakob disease: report of a postmortem case with review of the literature. *J Neurol Neurosurg Psychiatry* 2001; **70**: 696–699.
22. Asano M, Mohri S, Ironside JW, Ito M, Tamaoki N, Kitamoto T. vCJD prion acquires altered virulence through trans-species infection. *Biochem Biophys Res Commun* 2006; **342**: 293–299.
23. Kitamoto T, Shin RW, Doh-ura K *et al.* Abnormal isoform of prion proteins accumulates in the synaptic structures of the central nervous system in patients with Creutzfeldt-Jakob disease. *Am J Pathol* 1992; **140**: 1285–1294.
24. Kitamoto T, Muramoto T, Hilbich C, Beyreuther K, Tateishi J. N-terminal sequence of prion protein is also integrated into kuru plaques in patients with Gerstmann-Sträussler syndrome. *Brain Res* 1991; **545**: 319–321.
25. Kobayashi A, Asano M, Mohri S, Kitamoto T. Cross-sequence transmission of sporadic Creutzfeldt-Jakob disease creates a new prion strain. *J Biol Chem* 2007; **282**: 30022–30028.
26. Heinemann U, Krasnianski A, Meissner B *et al.* Creutzfeldt-Jakob disease in Germany: a prospective 12-year surveillance. *Brain* 2007; **130**: 1350–1359.
27. Kimberlin RH, Cole S, Walker CA. Temporary and permanent modifications to a single strain of mouse scrapie on transmission to rats and hamsters. *J Gen Virol* 1987; **68**: 1875–1881.

© 2009 Japanese Society of Neuropathology

JOURNAL OF VIROLOGY, Apr. 2010, p. 3230–3238 Vol. 84, No. 7
0022-538X/10/$12.00 doi:10.1128/JVI.02387-09
Copyright © 2010, American Society for Microbiology. All Rights Reserved.

Experimental Verification of a Traceback Phenomenon in Prion Infection[▽]

Atsushi Kobayashi,[1] Nobuyuki Sakuma,[1] Yuichi Matsuura,[2] Shirou Mohri,[2] Adriano Aguzzi,[3] and Tetsuyuki Kitamoto[1]*

Division of CJD Science and Technology, Department of Prion Research, Tohoku University Graduate School of Medicine, 2-1 Seiryo-machi, Aoba-ku, Sendai 980-8575, Japan[1]; Prion Disease Research Center, National Institute of Animal Health, Tsukuba, Ibaraki 305-0856, Japan[2]; and Institute of Neuropathology, University Hospital Zurich, CH-8002 Zurich, Switzerland[3]

Received 12 November 2009/Accepted 5 January 2010

The clinicopathological phenotypes of sporadic Creutzfeldt-Jakob disease (sCJD) correlate with the allelotypes (M or V) of the polymorphic codon 129 of the human prion protein (PrP) gene and the electrophoretic mobility patterns of abnormal prion protein (PrP^{Sc}). Transmission of sCJD prions to mice expressing human PrP with a heterologous genotype (referred to as cross-sequence transmission) results in prolonged incubation periods. We previously reported that cross-sequence transmission can generate a new prion strain with unique transmissibility, designated a traceback phenomenon. To verify experimentally the traceback of sCJD-VV2 prions, we inoculated sCJD-VV2 prions into mice expressing human PrP with the 129M/M genotype. These 129M/M mice showed altered neuropathology and a novel PrP^{Sc} type after a long incubation period. We then passaged the brain homogenate from the 129M/M mouse inoculated with sCJD-VV2 prions into other 129M/M or 129V/V mice. Despite cross-sequence transmission, 129V/V mice were highly susceptible to these prions compared to the 129M/M mice. The neuropathology and PrP^{Sc} type of the 129V/V mice inoculated with the 129M/M mouse-passaged sCJD-VV2 prions were identical to those of the 129V/V mice inoculated with sCJD-VV2 prions. Moreover, we generated for the first time a type 2 PrP^{Sc}-specific antibody in addition to type 1 PrP^{Sc}-specific antibody and discovered that drastic changes in the PrP^{Sc} subpopulation underlie the traceback phenomenon. Here, we report the first direct evidence of the traceback in prion infection.

Creutzfeldt-Jakob disease (CJD) is a lethal transmissible neurodegenerative disease caused by an abnormal isoform of prion protein (PrP^{Sc}), which is converted from the normal cellular isoform (PrP^{C}) (1, 23). The genotype (M/M, M/V, or V/V, where M and V are allelotypes) at polymorphic codon 129 of the human prion protein (PrP) gene and the type (type 1 or type 2) of PrP^{Sc} in the brain are major determinants of the clinicopathological phenotypes of sporadic CJD (sCJD) (15–18). Type 1 and type 2 PrP^{Sc} are distinguishable according to the size of the proteinase K-resistant core of PrP^{Sc} (PrP^{res}) (21 and 19 kDa, respectively), reflecting differences in the proteinase K cleavage site (at residues 82 and 97, respectively) (15, 18). According to this molecular typing system, sCJD can be classified into six subgroups (MM1, MM2, MV1, MV2, VV1, or VV2).

The homology of the PrP genes between inoculated animals and the inoculum determines the susceptibility to prion infection. Transmission of sCJD prions to mice expressing human PrP with a nonhomologous genotype (referred to as cross-sequence transmission) results in a relatively long incubation period (10, 12). Meanwhile, the cross-sequence transmission can generate a new prion strain. Transmission of sCJD-VV2 prions to mice expressing human PrP with the 129M/M genotype generates unusual PrP^{res} intermediate in size between type 1 and type 2 (10). We have designated this unusual PrP^{res} with an upward size shift (Sh+) from the inoculated type 2 template MM[VV2]2^{Sh+} PrP^{res}, where the notation is of the following form: host genotype [type of inoculated prion] type of generated PrP^{res}.

Similar to the MM[VV2]2^{Sh+} PrP^{res}, the intermediate-sized PrP^{res} has been observed in the plaque-type of dura mater graft-associated CJD (p-dCJD) (10, 13). Furthermore, a transmission study using p-dCJD prions revealed that PrP-humanized mice with the 129V/V genotype were highly susceptible to p-dCJD prions despite cross-sequence transmission (10). In addition, these 129V/V mice inoculated with p-dCJD prions produced type 2 PrP^{res} (10). These findings suggest that p-dCJD could be caused by cross-sequence transmission of sCJD-VV2 prions to individuals with the 129M/M genotype. We have designated this phenomenon "traceback." The traceback phenomenon was discovered for the first time by a transmission study using variant CJD (vCJD) prions (2). Mice expressing bovine PrP were highly susceptible to vCJD prions because vCJD was caused by cross-sequence transmission of bovine spongiform encephalopathy prions to human. These findings suggest that a traceback study can be a powerful tool to identify the origin of prions (2, 10, 11). However, the traceback phenomenon has not been verified experimentally despite the abundant circumstantial evidence described above.

To verify the traceback of sCJD-VV2 prions, we inoculated sCJD-VV2 prions into PrP-humanized mice with the 129M/M genotype as an experimental model of p-dCJD. Thereafter, we inoculated these MM[VV2]2^{Sh+} prions into PrP-humanized mice with the 129M/M or 129V/V genotype and compared the incubation period, neuropathology, and the type of PrP^{res} in the brain. Here, we report the first direct evidence of the traceback in prion infection.

* Corresponding author. Mailing address: Division of CJD Science and Technology, Department of Prion Research, Tohoku University Graduate School of Medicine, 2-1 Seiryo-machi, Aoba-ku, Sendai 980-8575, Japan. Phone: 81 22 717 8143. Fax: 81 22 717 8148. E-mail: kitamoto@mail.tains.tohoku.ac.jp.

▽ Published ahead of print on 20 January 2010.

TABLE 1. Primers used for the amplification of truncated human PrP gene fragments

Primer function and name	Sequence
Amplification of C-terminal truncation fragment	
BamHI-23	5′-GGATCCAAGAAGCGCCCGAAGCCTGGAGGA-3′
89-XhoI	5′-CTCGAGTCACCAGCCACCACCATGAGGCTG-3′
90-XhoI	5′-CTCGAGTCAACCCCAGCCACCACCATGAGG-3′
91-XhoI	5′-CTCGAGTCATTGACCCCAGCCACCACCATG-3′
92-XhoI	5′-CTCGAGTCATCCTTGACCCCAGCCACCACC-3′
93-XhoI	5′-CTCGAGTCAACCTCCTTGACCCCAGCCACC-3′
94-XhoI	5′-CTCGAGTCAGCCACCTCCTTGACCCCAGCC-3′
95-XhoI	5′-CTCGAGTCAGGTGCCACCTCCTTGACCCCA-3′
96-XhoI	5′-CTCGAGTCAGTGGGTGCCACCTCCTTGACC-3′
Amplification of N-terminal truncation fragment	
BamHI-82	5′-CGTGGATCCGGACAGCCTCATGGTGGTGGCTGG-3′
BamHI-84	5′-CGTGGATCCCCTCATGGTGGTGGCTGGGGTCAA-3′
BamHI-86	5′-CGTGGATCCGGTGGTGGCTGGGGTCAAGGAGGT-3′
BamHI-88	5′-CGTGGATCCGGCTGGGGTCAAGGAGGTGGCACC-3′
BamHI-90	5′-CGTGGATCCGGTCAAGGAGGTGGCACCCACAGT-3′
BamHI-92	5′-CGTGGATCCGGAGGTGGCACCCACAGTCAGTGG-3′
BamHI-94	5′-CGTGGATCCGGCACCCACAGTCAGTGGAACAAG-3′
BamHI-97	5′-CGTGGATCCAGTCAGTGGAACAAGCCGAGTAAG-3′
230-XhoI	5′-CCGCTCGAGTCACGATCCTCTCTGGTAATAGGCCTG-3′

MATERIALS AND METHODS

Production of PrP^{res} type-specific polyclonal antibodies. A synthetic peptide corresponding to human PrP residues 82 to 98 was used as the immunogen for type 1 PrP^{res}-specific antibody Tohoku 1 because residues 82 to 96 were retained in type 1 PrP^{res} but not in type 2 PrP^{res} after proteinase K digestion (18). For type 2 PrP^{res}-specific antibody Tohoku 2, a short synthetic peptide corresponding human PrP residues 97 to 103 was used as the immunogen because the length of the immunogen peptide is critical for the production of proteolytic cleavage site-specific polyclonal antibodies (25, 26). Cysteine residues were added to the C terminus of each peptide, which was utilized for conjugation to bovine thyroglobulin via EMCS [*N*-(6-maleimidocaproyloxy)succinimide] (Dojin). For the initial injection, 100 μg of conjugate was emulsified in complete Freund's adjuvant and subcutaneously injected into rabbits. For the boosting injections, 100 μg of conjugate was emulsified in incomplete Freund's adjuvant and was subcutaneously injected on days 7, 21, 35, 49, 63, 84, and 91. At day 98, the rabbits were sacrificed, and serum was collected. Antibodies were purified by affinity chromatography using the immunogen peptides. Another type 1 PrP^{res}-specific monoclonal antibody, POM2, reacts with repeated octapeptide epitopes 59 to 65, 67 to 73, 75 to 81, and 83 to 89 of human and murine PrP (21, 22).

Production of knock-in mice and transgenic mice. The production of knock-in mice expressing human PrP with 129M/M (Ki-Hu129M/M mice) and Ki-Hu129V/V mice has been reported previously (2). Ki-Hu129M/M mice and knock-in mice expressing human PrP with 129M/M and four octapeptide repeats (Ki-Hu129M_{4R}/M_{4R}) were crossed with transgenic mice expressing human PrP with 129M (Tg-Hu129M) and four octapeptide repeats (Tg-Hu129M_{4R}), respectively (10). The expression levels of human PrP in the brains from Tg+Ki-Hu129M/M and Tg+Ki-Hu129M_{4R}/M_{4R} mice were 1.2-fold and 9.8-fold, respectively, the levels observed in Ki-Hu129M/M mice.

Human brain inocula. Brain tissues were obtained at autopsy from CJD patients after informed consent for research use was received. The diagnosis of CJD and the type of PrP^{Sc} were confirmed by neuropathological examination, PrP^{Sc} immunohistochemistry, and Western blotting as described previously (7, 27). The genotype and the absence of mutations in the open reading frame of the PrP gene were determined by sequence analysis (8). The CJD cases selected for the transmission studies were typical of the sCJD-MM1 and sCJD-VV2 subgroups. In the sCJD-VV2 (AK) isolate, the plaque-type PrP deposition in the brain and the absence of periodic synchronous discharges on electroencephalogram were confirmed. More detailed information of the patient was reported previously (4). Isolates sCJD-MM1 (H3) and sCJD-VV2 (AK) showed the same levels of transmissibility to PrP-humanized mice as other sCJD-MM1 and sCJD-VV2 isolates, respectively (27).

Transmission experiments. Human brain homogenates (10%) and mouse brain homogenates (10%) were prepared as described previously (9). Intracerebral transmission was performed using 20 μl of the homogenates (27). The inoculated mice were sacrificed after the onset of disease, and their brains were immediately frozen or fixed in 10% buffered formalin.

Immunohistochemistry. Formalin-fixed mouse brains were treated with 60% formic acid for 1 h to inactivate the infectivity and then were embedded in paraffin. Tissue sections were pretreated by hydrolytic autoclaving before PrP immunohistochemistry (7). The N-terminal PrP (PrP-N) antiserum was used as the primary antibody (6). Goat anti-rabbit immunoglobulin polyclonal antibody labeled with the peroxidase-conjugated dextran polymer EnVision+ (Dako-Cytomation) was used as the secondary antibody.

Expression of a GST-recombinant PrP fusion protein. The open reading frame of the human PrP gene was amplified by PCR with human DNA. The amplified fragment was cloned into pBluescript plasmid (Stratagene). With the plasmid construct, N-terminally or C-terminally truncated human PrP gene fragments were amplified by PCR. The primers used for the amplification are shown in Table 1. These primers introduced BamHI sites at the 5′ end of the fragments and XhoI sites at the 3′ end of the fragments. The amplified fragments were cloned into pGEM-T Easy plasmid (Promega). After digestion with BamHI and XhoI, the fragments were inserted into the BamHI/XhoI sites of the expression vector pGEX-4T-1 (GE Healthcare). *Escherichia coli* BL21(DE3) cells were transformed with the pGEX-4T-1 plasmid constructs, and recombinant PrP fragments fused to glutathione *S*-transferase (GST) were purified using glutathione Sepharose 4B beads (GE Healthcare) according to the manufacturer's instructions. GST-tagged recombinant PrP fragments were subjected to 13% SDS-PAGE and Western blotting.

Enzyme-linked immunosorbent assay (ELISA). Synthetic peptides corresponding to human PrP residues 97 to 103 and 93 to 103 were used as the antigens. Plates were individually coated with 50 ng/50 μl/well antigen or with 0.1% bovine serum albumin (BSA). The polyclonal antibody Tohoku 2 was serially diluted and added to each well as the primary antibody. A goat anti-rabbit IgG Fab′ fraction labeled with horseradish peroxidase was used as the secondary antibody. The color was developed with o-phenylenediamine.

Western blotting. PrP^{Sc} was extracted from mouse brains with collagenase treatment as described previously (5) with some modifications. Samples were subjected to 13% SDS-PAGE and Western blotting as described previously (2). The monoclonal antibody 3F4 (Signet Laboratories), PrP-N (Immuno-Biological Laboratories), C-terminal PrP ([PrP-C] Immuno-Biological Laboratories), POM2, Tohoku 1, and Tohoku 2 were used as the primary antibodies. Anti-mouse EnVision+ and anti-rabbit EnVision+ were used as the secondary antibodies. The signal intensities of the Western blots were quantified with Quantity One software using a VersaDoc 5000 (Bio-Rad Laboratories) imaging device.

Statistical analysis. Incubation times and signal intensities of PrP^{res} bands are expressed as mean ± standard error of the mean (SEM).

TABLE 2. Transmission of sCJD prions to humanized mice with the 129M/M or 129V/V genotype

Inoculum	Incubation period (days [mean ± SEM]) in the indicated mouse strain[a]		
	Tg+Ki-Hu129M/M (1.2×)[b]	Ki-Hu129M/M (1×)[b]	Ki-Hu129V/V (1×)[b]
sCJD-MM1 (H3)	429 ± 6 (6/6)	467 ± 24 (8/8)	774 ± 32 (6/6)
sCJD-VV2 (AK)	723 ± 79 (4/4)	633 ± 49 (6/6)	312 ± 7 (4/4)
MM[VV2]2^{Sh+}	ND	685 ± 17 (6/6)	309 ± 3 (7/7)

[a] Values in parentheses are the number of diseased animals/number of inoculated animals. ND, not done.
[b] The expression level of human PrP in the brain.

RESULTS

Transmission of MM[VV2]2^{Sh+} prions to PrP-humanized mice with the 129M/M or 129V/V genotype. To verify the traceback of sCJD-VV2 prions, we performed intracerebral inoculation of a brain homogenate from as sCJD-VV2 patient into Tg+Ki-Hu129M/M mice. Thereafter, we performed the second passage of the brain homogenate from a Tg+Ki-Hu129M/M mouse inoculated with sCJD-VV2 prions (MM[VV2]2^{Sh+} prions). Since Tg+Ki-Hu129M/M mice were established before the Ki-Hu129M/M mice were produced, we used them in the primary transmission of sCJD-VV2 prions. The data of the primary transmission have been reported previously (10). The mean incubation time of Tg+Ki-Hu129M/M mice inoculated with sCJD-VV2 prions was 723 ± 79 days (number of diseased animals/number of inoculated animals, 4/4) (Table 2). In the second passage, we inoculated MM[VV2]2^{Sh+} prions intracerebrally into Ki-Hu129M/M mice or Ki-Hu129V/V mice. Ki-Hu129M/M mice inoculated with MM[VV2]2^{Sh+} prions showed long incubation times of 685 ± 17 days (6/6). In contrast, the mean incubation time of Ki-Hu129V/V mice inoculated with MM[VV2]2^{Sh+} prions was shortened to 309 ± 3 days (7/7). In spite of cross-sequence transmission, the mean incubation time of Ki-Hu129V/V mice was much shorter than that of Ki-Hu129M/M mice. Immunohistochemical analysis of the brains from Tg+Ki-Hu129M/M mice inoculated with sCJD-VV2 prions showed large plaque-type PrP deposits spread throughout the cerebral gray matter and thalamus (Fig. 1). Ki-Hu129M/M mice inoculated with MM[VV2]2^{Sh+} prions showed similar patterns of PrP deposition to those of Tg+Ki-Hu129M/M mice inoculated with sCJD-VV2 prions. In contrast, Ki-Hu129V/V mice inoculated with MM[VV2]2^{Sh+} prions showed diffuse synaptic-type PrP deposits in the gray matter and small plaque-type deposits restricted to the cerebral white matter. These patterns of PrP deposition were identical to those of Ki-Hu129V/V mice inoculated with sCJD-VV2 prions. Thus, we confirmed that Ki-Hu129V/V mice were highly susceptible to MM[VV2]2^{Sh+} prions that originated from sCJD-VV2 prions and that the neuropathology of Ki-Hu129V/V mice inoculated with MM[VV2]2^{Sh+} prions was identical to that of the Ki-Hu129V/V mice inoculated with the parental sCJD-VV2 prions.

Characterization of PrP^{res} in the mouse brains using PrP^{res} type-specific antibodies. Tg+Ki-Hu129M/M mice inoculated with sCJD-VV2 prions produced unusual PrP^{res} with an upward size shift from the inoculated type 2 template (10). To characterize these type 2^{Sh+} PrP^{res}, we produced PrP^{res} type-specific antibodies. Type 1 PrP^{res}-specific polyclonal antibody Tohoku 1 reacted with epitopes located between residues 82 and 96 of human PrP (Fig. 2). Type 2 PrP^{res}-specific polyclonal antibody Tohoku 2 reacted with a synthetic peptide corresponding to human PrP residues 97 to 103 (the immunogen peptide) but not with the peptide at residues 93 to 103 (Fig. 3). The amino group at the N terminus of the immunogen peptide might constitute an essential part of the epitopes for Tohoku 2, as reported in other proteolytic cleavage site-specific antibodies (25, 26). Therefore, Tohoku 1 should specifically detect type 1 PrP^{res}, and Tohoku 2 should specifically detect the N-terminal cleavage site of type 2 PrP^{res} after proteinase K digestion (Fig. 4A).

First, with these PrP^{res} type-specific antibodies, we performed Western blot analysis of the PrP^{res} in the human brain inocula used in this transmission study (Fig. 4B). In addition to the newly generated type-specific antibodies, we used the monoclonal antibody POM2, which also specifically detects

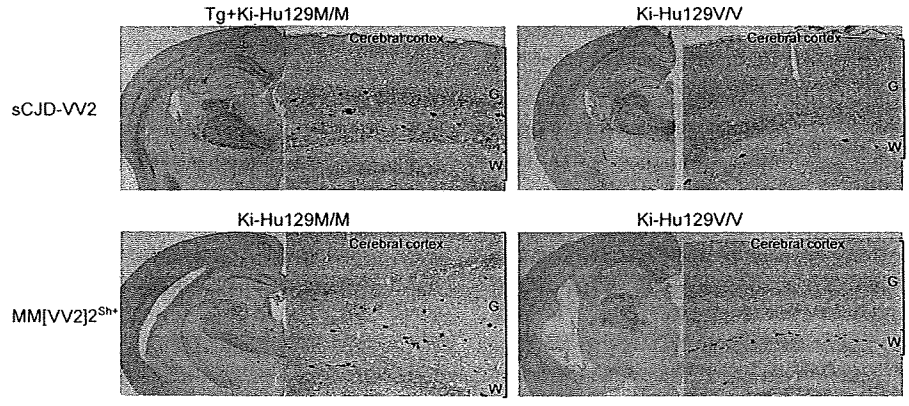

FIG. 1. The changes in neuropathology through cross-sequence transmission and traceback transmission. Immunohistochemical analysis of PrP^{Sc} in the brains from PrP-humanized mice inoculated with sCJD-VV2 prions or Tg+Ki-Hu129M/M mouse-passaged sCJD-VV2 prions. Tg+Ki-Hu129M/M mice inoculated with sCJD-VV2 prions or Ki-Hu129M/M mice inoculated with MM[VV2]2^{Sh+} prions showed prominent plaque-type PrP deposits throughout the cerebral gray matter. In contrast, plaque-type PrP deposits were restricted to within the white matter in the brains from Ki-Hu129V/V mice inoculated with sCJD-VV2 prions or MM[VV2]2^{Sh+} prions. G, gray matter; W, white matter.

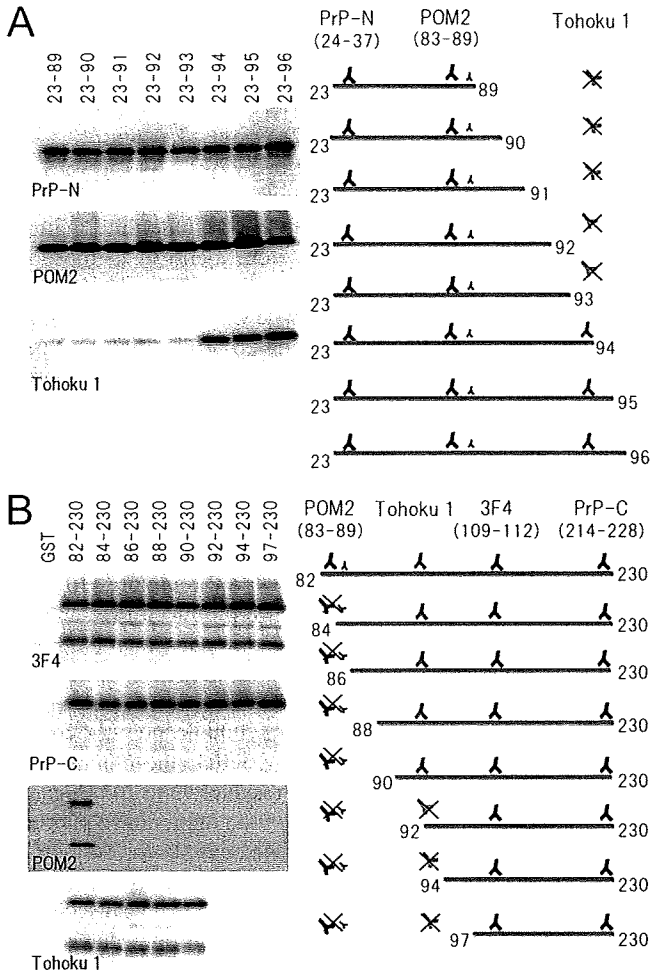

FIG. 2. Epitope mapping of polyclonal antibody Tohoku 1. (A) GST-tagged C-terminally truncated human PrP fragments were probed with PrP-N, POM2, or Tohoku 1. POM2 (21) reacted with all PrP fragments. In contrast, Tohoku 1 reacted with PrP fragments comprised of residues 23 to 94, 23 to 95, and 23 to 96. In addition, weak reactivity to PrP fragments 23 to 89, 23 to 90, 23 to 91, 23 to 92, and 23 to 93 was also observed. (B) GST-tagged N-terminally truncated human PrP fragments were probed with 3F4, PrP-C, POM2, or Tohoku 1. POM2 reacted with only the PrP fragment of residues 82 to 230. Tohoku 1 reacted with PrP fragments comprised of residues 82 to 230, 84 to 230, 86 to 230, 88 to 230, and 90 to 230. PrP residues 97 to 230, corresponding to proteinase K-digested type 2 PrP^{res} fragment, was not detected by Tohoku 1 or POM2. Low-molecular-weight bands lacking the PrP-C epitope should be degradation products. The reactivity of Tohoku 1 antibody (light blue), POM antibody (dark blue), and the other antibodies is summarized in a schematic diagram on the right.

type 1 PrP^{res} (Fig. 2) (21), as a reference antibody. Conventional typing of PrP^{res} using monoclonal antibody 3F4, which detects all PrP^{res} types, showed only a single PrP^{res} type in the brain of an sCJD-MM1 patient or in that of an sCJD-VV2 patient. With the PrP^{res} type-specific antibodies, however, small amounts of POM2/Tohoku 1-reactive subpopulations were observed in the sCJD-VV2 brain (Fig. 4B). The mean signal intensity of PrP^{res} in the sCJD-MM1 brain was assigned as 100/mm^2 in each experiment using 3F4, POM2, or Tohoku 1 (n = 3). In the Western blot analysis using 3F4, the mean signal intensity of PrP^{res} in the sCJD-VV2 brain was 224/mm^2 (Fig. 4B, white bars). In contrast, the signal intensities of POM2/Tohoku 1-reactive PrP^{res} bands in the sCJD-VV2 brain were 12/mm^2 (Fig. 4B, hatched bars) and 48/mm^2 (gray bars), respectively. Thus, using type 1 PrP^{res}-specific antibody, the sCJD-VV2 brain contained minority subpopulations that could be detected by type 1 PrP^{res}-specific antibodies, as reported previously (21, 28). The sizes of POM2/Tohoku 1-reactive bands were smaller than those of type 1 PrP^{res} in the sCJD-MM1 brain. Thus, POM2 and Tohoku 1 could detect the intermediate-sized PrP^{res} in addition to type 1 PrP^{res}. Furthermore, trace amounts of the Tohoku 2-reactive subpopulation were observed in the sCJD-MM1 brain (Fig. 4B, black bars). The mean signal intensity of PrP^{res} in the sCJD-VV2 brain was assigned as 100/mm^2 in each experiment using Tohoku 2 (n = 3). The mean signal intensity of Tohoku 2-reactive PrP^{res} bands in the sCJD-MM1 brain was 2/mm^2. Thus, using type 2 PrP^{res}-specific antibody, the minority type 2 PrP^{res} subpopulation could be detected even in the sCJD-MM1 brain.

Second, we performed Western blot analysis of PrP^{res} in the mouse brains using the PrP^{res} type-specific antibodies. Western blot analysis using 3F4 showed that Tg+Ki-Hu129M/M mice inoculated with sCJD-VV2 prions produced type 2^{Sh+} PrP^{res} that was located between type 1 PrP^{res} from Ki-Hu129M/M mice inoculated with sCJD-MM1 prions and type 2 PrP^{res} from Ki-Hu129V/V mice inoculated with sCJD-VV2 prions (Fig. 4C) (10). These PrP^{res} were probed with type-specific antibodies Tohoku 1, Tohoku 2, or POM2. The brains from Tg+Ki-Hu129M/M mice inoculated with sCJD-VV2 prions contained POM2/Tohoku 1-reactive PrP^{res} subpopulations in which the PrP^{res} were smaller than those of type 1 PrP^{res} from Ki-Hu129M/M inoculated with sCJD-MM1 prions. However, the signal intensities of these POM2/Tohoku 1-reactive bands were apparently decreased compared to those detected by 3F4 (Fig. 4C, bar graphs). The mean signal intensity of PrP^{res} from Ki-Hu129M/M mice inoculated with sCJD-MM1 prions was assigned as 100/mm^2 in each experiment using 3F4, POM2, or Tohoku 1 (n = 4). In the brains from Tg+Ki-Hu129M/M mice inoculated with sCJD-VV2 prions, the mean signal intensity of 3F4-reactive PrP^{res} bands was 154/mm^2 (white bars). However, the mean signal intensities of POM2/Tohoku 1-reactive PrP^{res} bands were 34/mm^2 (hatched bar) and 113/mm^2 (gray bar), respectively. Since more of the epitopes for Tohoku 1 were located at the C terminus than for POM2 (Fig. 2), the signal intensities of Tohoku 1-reactive bands might be higher than those of POM2-reactive bands. Thus, the brains from Tg+Ki-Hu129M/M mice inoculated with sCJD-VV2 prions contained the intermediate-sized PrP^{res}, but certain subpopulations that could not be detected by POM2 or Tohoku 1 must also have been present. The Tohoku 2-reactive subpopulation was not observed in Tg+Ki-Hu129M/M mice inoculated with sCJD-VV2 prions or Ki-Hu129M/M mice inoculated with sCJD-MM1 prions (Fig. 4C, black bars). The mean signal intensity of PrP^{res} from Ki-Hu129V/V mice inoculated with sCJD-VV2 prions was assigned as 100/mm^2 in each experiment using Tohoku 2 (n = 4). The brains from Ki-Hu129V/V mice inoculated with sCJD-VV2 prions contained small amounts of POM2/Tohoku 1-reactive subpopulations in addition to the Tohoku 2-reactive majority subpopulation. Thus, in the cross-sequence transmission of sCJD-VV2 prions to Tg+Ki-Hu129M/M mice, POM2/Tohoku 1-reactive subpopulations

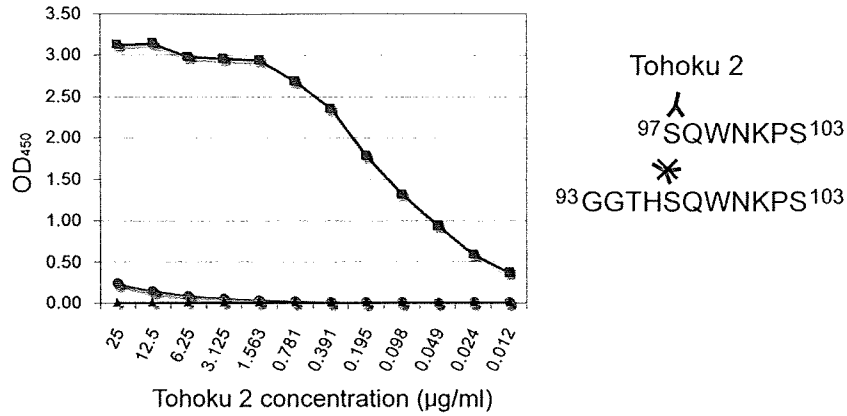

FIG. 3. Characterization of polyclonal antibody Tohoku 2 by peptide ELISA. Tohoku 2 specifically reacted with a synthetic peptide corresponding to human PrP residues 97 to 103 (■) but not with peptide at residues 93 to 103 (●). Control wells were coated with 0.1% BSA (▲). OD_{450}, optical density at 450 nm. The reactivity of Tohoku 2 antibody (pink) is summarized in a schematic diagram on the right. Tohoku 2 should recognize the N terminus of the human PrP fragment comprised of residues 97 to 103.

were increased, whereas the Tohoku 2 reactive-subpopulation was decreased. Therefore, the upward size shift from type 2 to type 2^{Sh+} in the Western blot analysis using 3F4 reflected the shift of the majority PrP^{res} subpopulation from the Tohoku 2-reactive subpopulation to the POM2/Tohoku 1-reactive subpopulation.

In the second passage of the brain homogenate from Tg+Ki-Hu129M/M mouse inoculated with sCJD-VV2 prions (MM[VV2]2^{Sh+} prions: host genotype [type of inoculated prions] type of generated PrP^{res}), Ki-Hu129M/M mice inoculated with MM[VV2]2^{Sh+} prions produced the intermediate-sized PrP^{res} that were identical in size to parental MM[VV2]2^{Sh+} prions when probed with 3F4 (Fig. 4C). Similar to the brains from Tg+Ki-Hu129M/M mice inoculated with sCJD-VV2 prions, the brains from Ki-Hu129M/M mice inoculated with MM[VV2]2^{Sh+} prions contained POM2/Tohoku 1-reactive subpopulations but not the Tohoku 2-reactive subpopulation. In the brains from Ki-Hu129M/M mice inoculated with MM[VV2]2^{Sh+} prions, the mean signal intensities of 3F4, POM2, and Tohoku 1-reactive PrP^{res} bands were 176/mm^2 (Fig. 4C, white bars), 85/mm^2 (hatched bars), and 139/mm^2 (gray bars), respectively. Meanwhile, Western blot analysis using 3F4 showed that Ki-Hu129V/V mice inoculated with MM[VV2]2^{Sh+} prions produced type 2 PrP^{res}; i.e., the intermediate-sized PrP^{res} reverted to type 2 when MM[VV2]2^{Sh+} prions were transmitted to Ki-Hu129V/V mice. Moreover, in the traceback transmission of MM[VV2]2^{Sh+} prions to Ki-Hu129V/V mice, POM2/Tohoku 1-reactive subpopulations were decreased, whereas the Tohoku 2 reactive-subpopulation predominated. In the brains from Ki-Hu129V/V mice inoculated with MM[VV2]2^{Sh+} prions, the mean signal intensities of 3F4, POM2, and Tohoku 1-reactive PrP^{res} bands were 179/mm^2 (Fig. 4C, white bars), 13/mm^2 (hatched bars), and 43/mm^2 (gray bars), respectively, whereas the mean signal intensity of the Tohoku 2-reactive PrP^{res} bands was 159/mm^2 (black bars). Thus, PrP^{res} type-specific antibodies revealed that cross-sequence transmission of sCJD-VV2 prions generated a new prion strain (MM[VV2]2^{Sh+} prions) with an altered proportion of PrP^{res} subpopulations and that the altered proportion reverted to the original proportion through the traceback transmission to Ki-Hu129V/V mice.

Traceback study of p-dCJD prions reevaluated with the PrP^{res} type-specific antibodies. We reported previously that p-dCJD prions showed the intermediate-sized PrP^{res}, and that Ki-Hu129V/V mice inoculated with p-dCJD prions showed accumulation of type 2 PrP^{res} (10). To characterize these PrP^{res} in the brains from PrP-humanized mice inoculated with p-dCJD prions, we performed Western blot analysis using PrP^{res} type-specific antibodies (Fig. 5). Since Tg+Ki-Hu129M_{4R}/M_{4R} mice were already established before the Ki-Hu129M/M mice were produced, we used them in the traceback study of p-dCJD or nonplaque-type dCJD (np-dCJD) prions. Subsequently, we confirmed that Tg+Ki-Hu129M_{4R}/M_{4R}, Ki-Hu129M/M, and Tg+Ki-Hu129M/M mice produced PrP^{res} identical in size in the transmission studies using various CJD prions (10). POM2/Tohoku 1-reactive subpopulations existed in the brains from Tg+Ki-Hu129M_{4R}/M_{4R} mice inoculated with p-dCJD prions, but the signal intensities were apparently decreased compared to those detected by 3F4 (Fig. 5). The mean signal intensity of PrP^{res} from Tg+Ki-Hu129M_{4R}/M_{4R} mice inoculated with sCJD-MM1 prions was assigned as 100/mm^2 in each experiment using 3F4, POM2, or Tohoku 1 (n = 3). In the brains from Tg+Ki-Hu129M_{4R}/M_{4R} mice inoculated with p-dCJD prions, the mean signal intensity of 3F4-reactive PrP^{res} bands was 105/mm^2 (Fig. 5, white bars). However, the mean signal intensities of POM2/Tohoku 1-reactive PrP^{res} bands were 23/mm^2 (hatched bars) and 45/mm^2 (gray bars), respectively. The POM2/Tohoku 1-reactive bands were smaller than those of type 1 PrP^{res} from Tg+Ki-Hu129M_{4R}/M_{4R} mice inoculated with np-dCJD prions or sCJD-MM1 prions. In addition, trace amounts of the Tohoku 2-reactive subpopulation were observed in the brains from Tg+Ki-Hu129M_{4R}/M_{4R} mice inoculated with p-dCJD prions, np-dCJD prions, or sCJD-MM1 prions (Fig. 5, black bars). The mean signal intensity of PrP^{res} from Ki-Hu129V/V mice inoculated with sCJD-VV2 prions was assigned as 100/mm^2 in each experiment using Tohoku 2 (n = 3). Since the sizes of these Tohoku 2-reactive bands were identical to those of

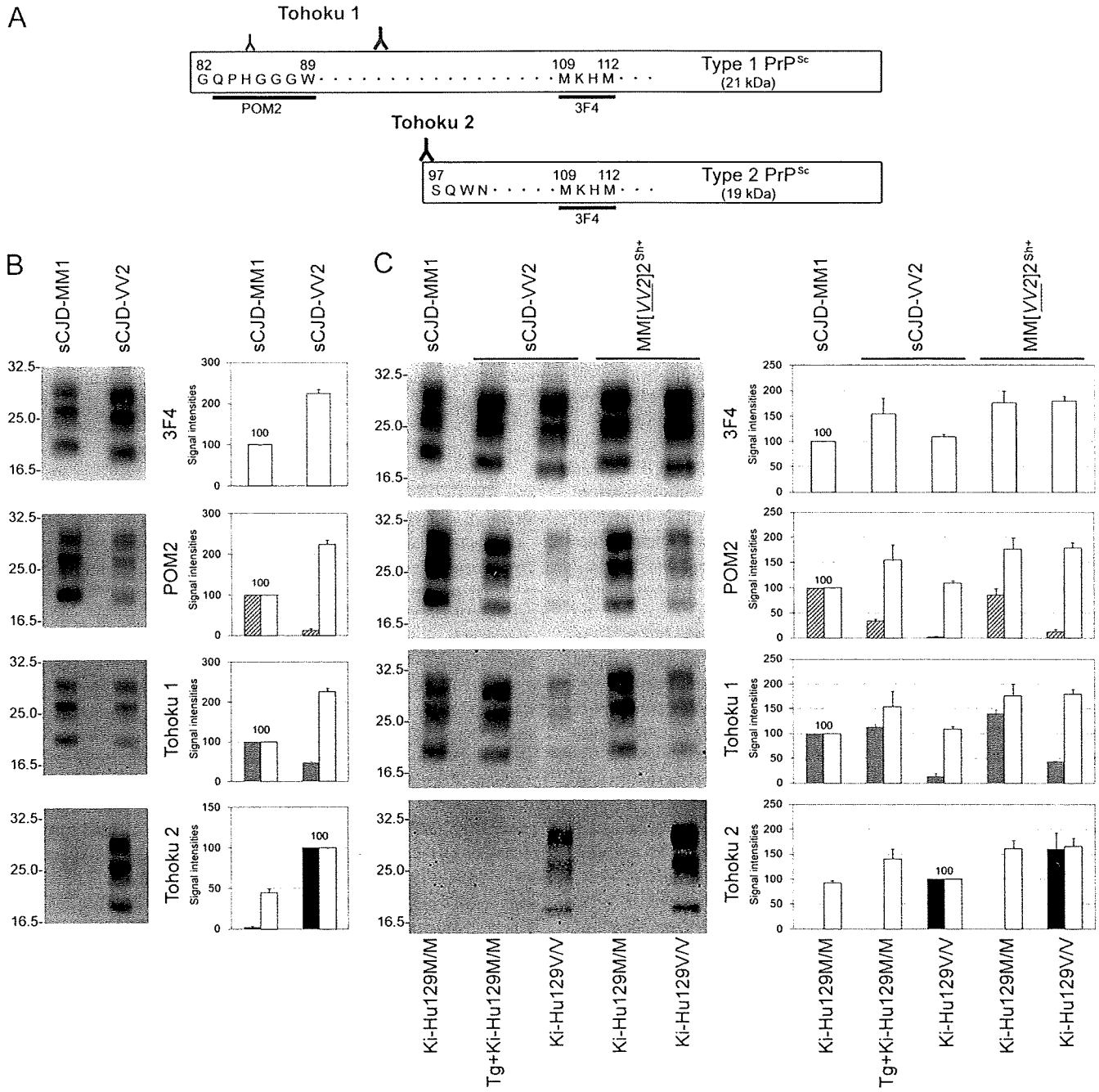

FIG. 4. Characterization of PrP^{res} using PrP^{res} type-specific antibodies. (A) The epitopes for type 1 PrP^{res}-specific polyclonal antibody Tohoku 1 (grey) or type 2 PrP^{res}-specific polyclonal antibody Tohoku 2 (black) are summarized in a schematic diagram. POM2 also specifically detects type 1 PrP^{res} (21). 3F4 detects all types of PrP^{res}. (B) Characterization of the human brain inocula used for the transmission studies. Western blot analysis using POM2 and Tohoku 1 revealed that the sCJD-VV2 brain contained minority subpopulations that could be detected by type 1 PrP^{res}-specific antibodies, as reported previously (21, 28). Meanwhile, using type 2 PrP^{res}-specific antibody Tohoku 2, the minority type 2 PrP^{res} subpopulation could be detected even in the sCJD-MM1 brain. The mean signal intensity of PrP^{res} in the sCJD-MM1 brain was assigned as 100/mm^2 in each experiment using 3F4 (white bars), POM2 (hatched bars), or Tohoku 1 (gray bars). The mean signal intensity of PrP^{res} in the sCJD-VV2 brain was assigned as 100/mm^2 in each experiment using Tohoku 2. The signal intensities of PrP^{res} are expressed as mean ± SEM (n = 3). (C) Western blot analysis using PrP^{res} type-specific antibodies revealed that drastic changes in the PrP^{res} subpopulations underlie the traceback phenomenon. In the cross-sequence transmission of sCJD-VV2 prions to Tg+Ki-Hu129M/M mice, POM2/Tohoku 1-reactive subpopulations were increased, whereas the Tohoku 2 reactive-subpopulation was decreased. Conversely, in the traceback transmission of MM[VV2]2^{Sh+} prions to Ki-Hu129V/V mice, POM2/Tohoku 1-reactive subpopulations were decreased, whereas the Tohoku 2 reactive-subpopulation predominated. The signal intensity of PrP^{res} from Ki-Hu129M/M mice inoculated with sCJD-MM1 was assigned as 100/mm^2 in each experiment using 3F4 (white bars), POM2 (hatched bars), or Tohoku 1 (gray bars). The signal intensity of PrP^{res} from Ki-Hu129V/V mice inoculated with sCJD-VV2 was assigned as 100/mm^2 in each experiment using Tohoku 2 (black bars). The signal intensity of PrP^{res} is expressed as the mean ± SEM (n = 4).

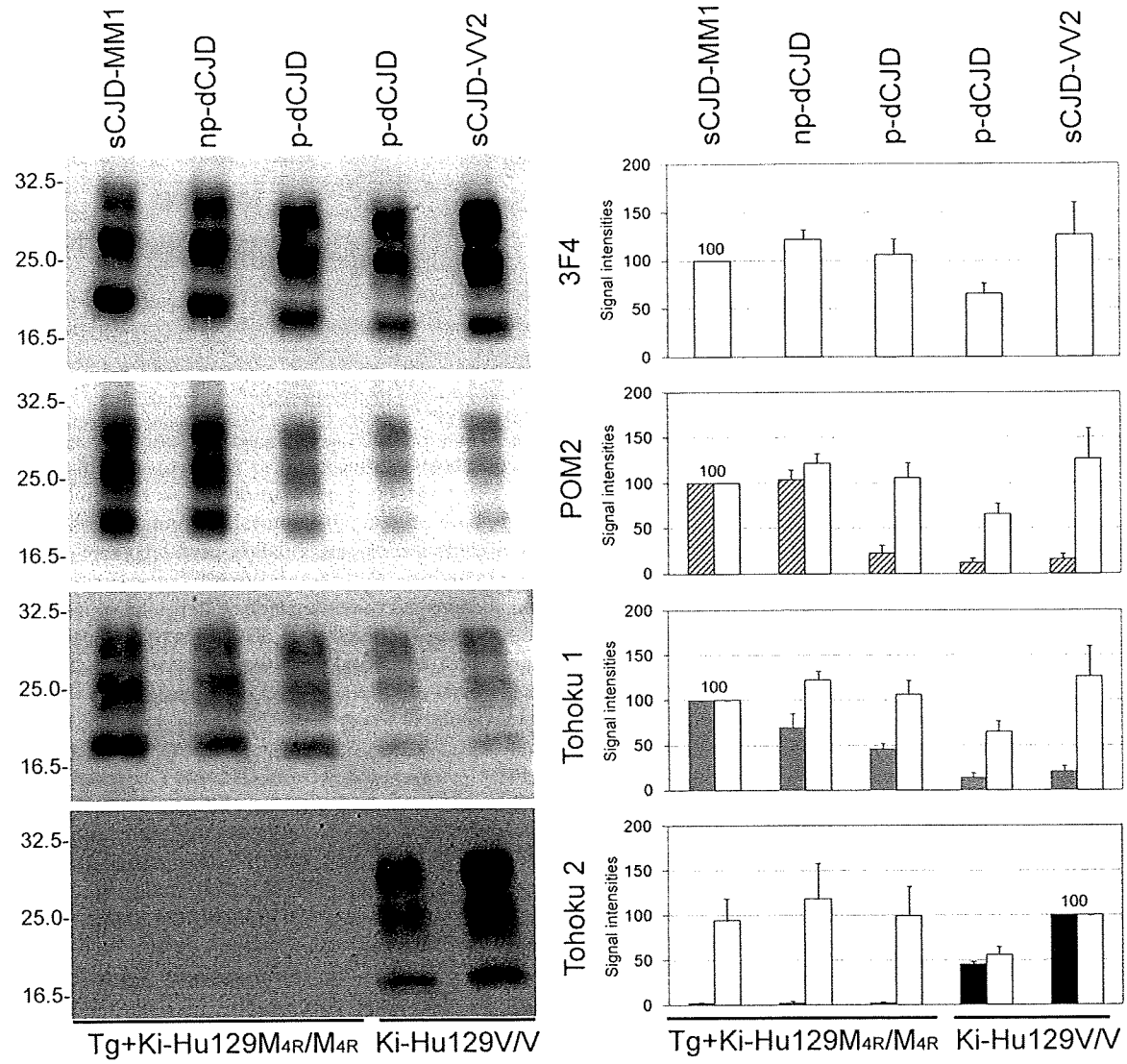

FIG. 5. Traceback study of p-dCJD prions reevaluated with PrP^{res} type-specific antibodies. In the traceback transmission of p-dCJD prions to Ki-Hu129V/V mice, POM2/Tohoku 1-reactive subpopulations were decreased, whereas the Tohoku 2 reactive-subpopulation predominated. In addition, trace amounts of the Tohoku 2-reactive subpopulation were observed in the brains from Tg+Ki-Hu129M_{4R}/M_{4R} mice inoculated with p-dCJD prions, np-dCJD prions, or sCJD-MM1 prions. The signal intensity of PrP^{res} from Tg+Ki-Hu129M_{4R}/M_{4R} mice inoculated with sCJD-MM1 was assigned as 100/mm^2 in each experiment using 3F4 (white bars), POM2 (hatched bars), or Tohoku 1 (gray bars). The signal intensity of PrP^{res} from Ki-Hu129V/V mice inoculated with sCJD-VV2 was assigned as 100/mm^2 in each experiment using Tohoku 2 (black bars). The signal intensity of PrP^{res} is expressed as the mean ± SEM (n = 3).

type 2 PrP^{res} from Ki-Hu129V/V mice inoculated with sCJD-VV2 prions, Tohoku 2 could specifically detect type 2 PrP^{res}. Meanwhile, in the transmission of p-dCJD prions to Ki-Hu129V/V mice, POM2/Tohoku 1-reactive subpopulations were decreased, whereas the Tohoku 2-reactive subpopulation predominated. In the brains from Ki-Hu129V/V mice inoculated with p-dCJD prions, the mean signal intensities of 3F4, POM2, and Tohoku 1-reactive PrP^{res} bands were 65/mm^2 (Fig. 5, white bars), 12/mm^2 (hatched bars), and 13/mm^2 (gray bars), respectively, whereas the mean signal intensity of Tohoku 2-reactive PrP^{res} bands was 45/mm^2 (black bars). Thus, the changes in PrP^{res} subpopulation observed in this traceback study of p-dCJD prions were identical to those observed in the traceback study of MM[VV2]2^{Sh+} prions.

DISCUSSION

In order to protect humans and animals from infectious diseases, it is often crucial to determine the origin of the isolates that may lie at the origin of epidemics. In the case of conventional pathogens, this is relatively simple and primarily involves the sequencing of pathogen-associated nucleic acids. Because prions lack informational nucleic acids, however, the unambiguous assignment of a given infection to a specific source is very often impossible. Therefore, methods aimed at characterizing stable prion properties after passaging through hosts would be extremely valuable.

Here, we demonstrate the first direct evidence of traceback in prion infection. Ki-Hu129V/V mice were highly susceptible

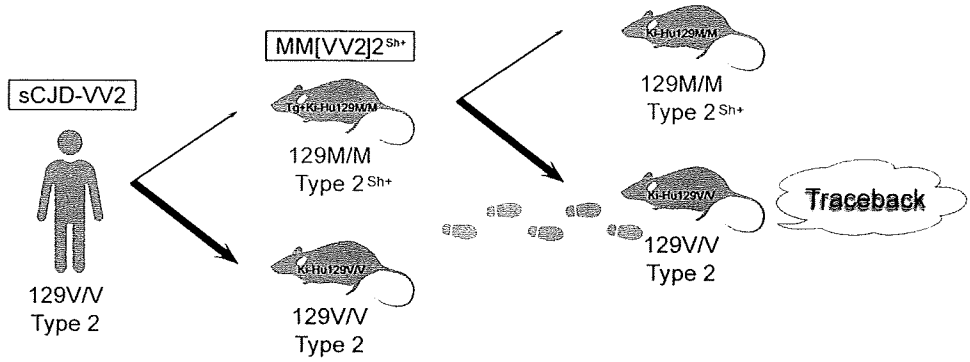

FIG. 6. Diagram of the traceback studies. The cross-sequence transmission of sCJD-VV2 prions to Tg+Ki-Hu129M/M mice generated a new prion strain (MM[VV2]2^{Sh+} prions) with altered conformational properties and disease phenotypes after a long incubation period. In the secondary transmission, Ki-Hu129V/V mice were highly susceptible to these MM[VV2]2^{Sh+} prions despite cross-sequence transmission. Furthermore, the altered conformational properties and disease phenotypes reverted to the original ones. If atypical prion strains emerge through cross-sequence transmission, traceback studies can be a reliable tool to identify the origin of prions.

to the Tg+Ki-Hu129M/M mouse-passaged sCJD-VV2 prions (MM[VV2]2^{Sh+} prions) despite cross-sequence transmission (Fig. 6). In addition, MM[VV2]2^{Sh+} prions and sCJD-VV2 prions exhibited similar neuropathologies and the identical PrP^{res} types when inoculated into Ki-Hu129V/V mice; i.e., the altered disease phenotypes and unusual PrP^{res} type of MM[VV2]2^{Sh+} prions reverted to those of the parental sCJD-VV2 prions. Furthermore, we generated for the first time type 2 PrP^{res}-specific polyclonal antibody Tohoku 2 in addition to type 1 PrP^{res}-specific polyclonal antibody Tohoku 1. These PrP^{res} type-specific antibodies revealed that drastic changes in the PrP^{res} subpopulations underlie the traceback phenomenon.

The present study clearly shows that traceback studies can be a reliable tool to identify the origin of prions if atypical prion strains emerge through cross-sequence transmission. Although the numbers of animals and human brain inocula used for the transmission were limited in the present study, we demonstrated experimentally the traceback phenomenon: Ki-Hu129V/V mice were highly susceptible to MM[VV2]2^{Sh+} prions that originated from sCJD-VV2 prions. In the cross-sequence transmission of sCJD-VV2 prions to Tg+Ki-Hu129M/M mice, POM2/Tohoku 1-reactive subpopulations were increased, whereas the Tohoku 2-reactive subpopulation was decreased. In contrast, the altered proportion of PrP^{res} subpopulations reverted to the original proportion through the traceback transmission to Ki-Hu129V/V mice. Similar changes in the PrP^{res} subpopulations were observed in the traceback transmission of p-dCJD prions to Ki-Hu129V/V mice. Therefore, the present study shows again that p-dCJD could be caused by cross-sequence transmission of sCJD-VV2 prions to individuals with the 129M/M genotype.

The drastic changes in the PrP^{res} subpopulations can be the molecular basis of the traceback phenomena. We suppose that the subpopulation change observed in the cross-sequence transmission is due to adaptation and/or a selection process (3, 20), which requires a relatively long incubation period. In contrast, the subpopulation change observed in the traceback transmission might be due to reemergence of the parental prions. Since the emerging prion strain generated by the cross-sequence transmission retains the memory of the parental prions within its conformational properties or repertoire of PrP^{Sc} subpopulations, the parental PrP^{Sc} subpopulation reemerges and becomes predominant if the emerging prion strain is transmitted to the original host. Therefore, the incubation period can be shortened, and the altered disease phenotypes revert to the original ones in traceback transmission.

Unexpectedly, type 2 PrP^{res}-specific antibody Tohoku 2 revealed that trace amounts of type 2 PrP^{res} coexisted with type 1 PrP^{res} in the brain of an sCJD-MM1 patient. In addition, PrP-humanized mice with the 129M/M genotype inoculated with sCJD-MM1 prions could produce trace amounts of type 2 PrP^{res} in addition to type 1 PrP^{res}. The additional type 2 PrP^{res} was detected in Tg+Ki-Hu129M_{4R}/M_{4R} but not in Ki-Hu129M/M mice. Since Tg+Ki-Hu129M_{4R}/M_{4R} mice express human PrP with four octapeptide repeats at 9.8-fold the level observed in Ki-Hu129M/M mice, these differences might account for the subtle change. Further large-scale studies are needed to determine whether an additional type 2 PrP^{res} can be detected by Tohoku 2 in other human CJD cases formerly classified as type 1.

The present study raises the possibility that cooccurrence of multiple PrP^{res} subpopulations in the same brain might be a general phenomenon. Both type 1 and type 2 PrP^{res} can be detected in the same brain in 35% of sCJD patients examined (19, 24). By using type 1 PrP^{res}-specific antibodies, the minority type 1 subpopulation can be detected with type 2 in all sCJD patients or variant CJD patients formerly classified as type 2 (21, 28). In accord with these reports, small amounts of type 1 (and the intermediate-sized) PrP^{res} were detected by type 1 PrP^{res}-specific antibodies in Ki-Hu129V/V mice inoculated with sCJD-VV2 prions in the present study. In addition, trace amounts of type 2 PrP^{res} were detected by type 2 PrP^{res}-specific antibody in the sCJD-MM1 patient or Tg+Ki-Hu129M_{4R}/M_{4R} mice inoculated with sCJD-MM1 prions. These findings are in line with a report that diverse PrP^{res} fragments can be detected by N-terminal amino acid sequencing in the same brain even though only a single PrP^{res} type is detected by conventional Western blot analysis (18). Since the conventional Western blot analysis using antibodies that react with all PrP^{res} types failed to detect type 1 PrP^{res} unless type 1 PrP^{res} represented more than 30 to 40% of total PrP^{res} in experimentally mixed

type 1 and type 2 brain samples, the cooccurrence of multiple PrP^{res} subpopulations might be underestimated (21, 28). Therefore, the "type" of PrP^{Sc} determined by the conventional typing system might merely represent the predominant PrP^{res} subpopulation among multiple subpopulations.

However, the biological importance of the minority PrP^{res} subpopulation detected by the PrP^{res} type-specific antibodies or by N-terminal amino acid sequencing remains to be determined. Insufficient proteinase K digestion can generate type 1-specific antibody-reactive PrP bands in brain samples from sCJD or vCJD patients classified as type 2 (14). Otherwise, the size of the PrP^{res} fragment might not always reflect the conformation of PrP^{Sc}; e.g., the minority MM1 PrP^{res} subpopulation detected in sCJD-MM2 patients might differ from the genuine MM1 PrP^{res} of sCJD-MM1 patients. It remains unknown whether the minority PrP^{res} subpopulation has infectivity and pathogenicity to cause prion disease. A concise and attractive explanation would be that the proportion of PrP^{Sc} subpopulations in the brain determines the disease phenotype, transmissibility, and the type of PrP^{Sc} determined by the conventional typing system, but further studies are needed to elucidate why multiple PrP^{res} subpopulations can be detected in the same brain. Therefore, the significance of the conventional molecular typing system using antibodies that react with all PrP^{res} types is likely to continue to be used in the classification of sCJD.

In conclusion, we verified experimentally that traceback studies can be a reliable tool to identify the origin of prions. The present study shows that the changes in PrP^{res} subpopulations correlate with the changes in prion strain-specific properties, e.g., transmissibility and disease phenotypes, in the traceback transmission. Hereafter, the proportion of PrP^{res} subpopulations in human CJD cases should be analyzed quantitatively using the PrP^{res} type-specific antibodies Tohoku 1 and Tohoku 2.

ACKNOWLEDGMENTS

We thank Y. Ishikawa, H. Kudo and K. Abe for excellent technical assistance and B. Bell for critical review of the manuscript.

This study was supported by the Program for Promotion of Fundamental Studies in Health Sciences of National Institute of Biomedical Innovation (S.M. and T.K.), a Grant-in-Aid from the Ministry of Health, Labor and Welfare (A.K., S.M., and T.K.), and a Grant-in-Aid for Scientific Research from the Ministry of Education, Culture, Sports, Science and Technology (A.K. and T.K.).

REFERENCES

1. **Aguzzi, A., and A. M. Calella.** 2009. Prions: protein aggregation and infectious diseases. Physiol. Rev. **89:**1105–1152.
2. **Asano, M., S. Mohri, J. W. Ironside, M. Ito, N. Tamaoki, and T. Kitamoto.** 2006. vCJD prion acquires altered virulence through trans-species infection. Biochem. Biophys. Res. Commun. **342:**293–299.
3. **Collinge, J., and M. R. Scott.** 2007. A general model of prion strains and their pathogenicity. Science **318:**930–936.
4. **Fukushima, R., Y. Shiga, M. Nakamura, J. Fujimori, T. Kitamoto, and Y. Yoshida.** 2004. MRI characteristics of sporadic CJD with valine homozygosity at codon 129 of the prion protein gene and PrP^{Sc} type 2 in Japan. J. Neurol. Neurosurg. Psychiatry **75:**485–487.
5. **Grathwohl, K. U. D., M. Horiuchi, N. Ishiguro, and M. Shinagawa.** 1996. Improvement of PrP^{Sc}-detection in mouse spleen early at the preclinical stage of scrapie with collagenase-completed tissue homogenization and Sarkosyl-NaCl extraction of PrP^{Sc}. Arch. Virol. **141:**1863–1874.
6. **Kitamoto, T., T. Muramoto, C. Hilbich, K. Beyreuther, and J. Tateishi.** 1991. N-terminal sequence of prion protein is also integrated into kuru plaques in patients with Gerstmann-Sträussler syndrome. Brain Res. **545:**319–321.
7. **Kitamoto, T., R. W. Shin, K. Doh-ura, N. Tomokane, M. Miyazono, T. Muramoto, and J. Tateishi.** 1992. Abnormal isoform of prion proteins accumulates in the synaptic structures of the central nervous system in patients with Creutzfeldt-Jakob disease. Am. J. Pathol. **140:**1285–1294.
8. **Kitamoto, T., M. Ohta, K. Doh-ura, S. Hitoshi, Y. Terao, and J. Tateishi.** 1993. Novel missense variants of prion protein in Creutzfeldt-Jakob disease or Gerstmann-Sträussler syndrome. Biochem. Biophys. Res. Commun. **191:**709–714.
9. **Kitamoto, T., S. Mohri, J. W. Ironside, I. Miyoshi, T. Tanaka, N. Kitamoto, S. Itohara, N. Kasai, M. Katsuki, J. Higuchi, T. Muramoto, and R. W. Shin.** 2002. Follicular dendritic cell of the knock-in mouse provides a new bioassay for human prions. Biochem. Biophys. Res. Commun. **294:**280–286.
10. **Kobayashi, A., M. Asano, S. Mohri, and T. Kitamoto.** 2007. Cross-sequence transmission of sporadic Creutzfeldt-Jakob disease creates a new prion strain. J. Biol. Chem. **282:**30022–30028.
11. **Kobayashi, A., M. Asano, S. Mohri, and T. Kitamoto.** 2009. A traceback phenomenon can reveal the origin of prion infection. Neuropathology **29:**619–624.
12. **Korth, C., K. Kaneko, D. Groth, N. Heye, G. Telling, J. Mastrianni, P. Parchi, P. Gambetti, R. Will, J. Ironside, C. Heinrich, P. Tremblay, S. J. DeArmond, and S. B. Prusiner.** 2003. Abbreviated incubation times for human prions in mice expressing a chimeric mouse-human prion protein transgene. Proc. Natl. Acad. Sci. U. S. A. **100:**4784–4789.
13. **Kretzschmar, H. A., S. Sethi, Z. Földvári, O. Windl, V. Querner, I. Zerr, and S. Poser.** 2003. Iatrogenic Creutzfeldt-Jakob disease with florid plaques. Brain Pathol. **13:**245–249.
14. **Notari, S., S. Capellari, J. Langeveld, A. Giese, R. Strammiello, P. Gambetti, H. A. Kretzschmar, and P. Parchi.** 2007. A refined method for molecular typing reveals that co-occurrence of PrP^{Sc} types in Creutzfeldt-Jakob disease is not the rule. Lab. Invest. **87:**1103–1112.
15. **Parchi, P., R. Castellani, S. Capellari, B. Ghetti, K. Young, S. G. Chen, M. Farlow, D. W. Dickson, A. A. F. Sima, J. Q. Trojanowski, R. B. Petersen, and P. Gambetti.** 1996. Molecular basis of phenotypic variability in sporadic Creutzfeldt-Jakob disease. Ann. Neurol. **39:**767–778.
16. **Parchi, P., S. Capellari, S. G. Chen, R. B. Petersen, P. Gambetti, N. Kopp, P. Brown, T. Kitamoto, J. Tateishi, A. Giese, and H. Kretzschmar.** 1997. Typing prion isoforms. Nature **386:**232–234.
17. **Parchi, P., A. Giese, S. Capellari, P. Brown, W. Schulz-Schaeffer, O. Windl, I. Zerr, H. Budka, N. Kopp, P. Piccardo, S. Poser, A. Rojiani, N. Streichemberger, J. Julien, C. Vital, B. Ghetti, P. Gambetti, and H. Kretzschmar.** 1999. Classification of sporadic Creutzfeldt-Jakob disease based on molecular and phenotypic analysis of 300 subjects. Ann. Neurol. **46:**224–233.
18. **Parchi, P., W. Zou, W. Wang, P. Brown, S. Capellari, B. Ghetti, N. Kopp, W. J. Schulz-Schaeffer, H. A. Kretzschmar, M. W. Head, J. W. Ironside, P. Gambetti, and S. G. Chen.** 2000. Genetic influence on the structural variations of the abnormal prion protein. Proc. Natl. Acad. Sci. U. S. A. **97:**10168–10172.
19. **Parchi, P., R. Strammiello, S. Notari, A. Giese, J. P. M. Langeveld, A. Ladogana, I. Zerr, F. Roncaroli, P. Cras, B. Ghetti, M. Pocchiari, H. Kretzschmar, and S. Capellari.** 29 August 2009. Incidence and spectrum of sporadic Creutzfeldt-Jakob disease variants with mixed phenotype and co-occurrence of PrP^{Sc} types: an updated classification. Acta Neuropathol. doi:10.1007/s00401-009-0585-1.
20. **Peretz, D., R. A. Williamson, G. Legname, Y. Matsunaga, J. Vergara, D. R. Burton, S. J. DeArmond, S. B. Prusiner, and M. R. Scott.** 2002. A change in the conformation of prions accompanies the emergence of a new prion strain. Neuron **34:**921–932.
21. **Polymenidou, M., K. Stoeck, M. Glatzel, M. Vey, A. Bellon, and A. Aguzzi.** 2005. Coexistence of multiple PrPSc types in individuals with Creutzfeldt-Jakob disease. Lancet Neurol. **4:**805–814.
22. **Polymenidou, M., R. Moos, M. Scott, C. Sigurdson, Y. Z. Shi, B. Yajima, I. Hafner-Bratkovic, R. Jerala, S. Hornemann, K. Wuthrich, A. Bellon, M. Vey, G. Garen, M. N. James, N. Kav, and A. Aguzzi.** 2008. The POM monoclonals: a comprehensive set of antibodies to non-overlapping prion protein epitopes. PLoS One **3:**e3872.
23. **Prusiner, S. B., M. R. Scott, J. P. DeArmond, and F. E. Cohen.** 1998. Prion protein biology. Cell **93:**337–348.
24. **Puoti, G., G. Giaccone, G. Rossi, B. Canciani, O. Bugiani, and F. Tagliavini.** 1999. Sporadic Creutzfeldt-Jakob disease: co-occurrence of different types of PrP^{Sc} in the same brain. Neurology **53:**2173–2176.
25. **Saido, T. C., S. Nagao, M. Shiramine, M. Tsukaguchi, H. Sorimachi, H. Murofushi, T. Tsuchiya, H. Ito, and K. Suzuki.** 1992. Autolytic transition of μ-calpain upon activation as resolved by antibodies distinguishing between the pre- and post-autolysis forms. J. Biochem. **111:**81–86.
26. **Saido, T. C., T. Iwatsubo, D. M. A. Mann, H. Shimada, Y. Ihara, and S. Kawashima.** 1995. Dominant and differential deposition of distinct β-amyloid peptide species, $A\beta_{N3(pE)}$, in senile plaques. Neuron **14:**457–466.
27. **Taguchi, Y., S. Mohri, J. W. Ironside, T. Muramoto, and T. Kitamoto.** 2003. Humanized knock-in mice expressing chimeric prion protein showed varied susceptibility to different human prions. Am. J. Pathol. **163:**2585–2593.
28. **Yull, H. M., D. L. Ritchie, J. P. M. Langeveld, F. G. van Zijderveld, M. E. Bruce, J. W. Ironside, and M. W. Head.** 2006. Detection of type 1 prion protein in variant Creutzfeldt-Jakob disease. Am. J. Pathol. **168:**151–157.

Biochemical and Biophysical Research Communications 391 (2010) 1681–1686

Contents lists available at ScienceDirect

Biochemical and Biophysical Research Communications

journal homepage: www.elsevier.com/locate/ybbrc

Amino acid conditions near the GPI anchor attachment site of prion protein for the conversion and the GPI anchoring

Masaki Hizume [a,b], Atsushi Kobayashi [a], Hidehiro Mizusawa [b], Tetsuyuki Kitamoto [a,*]

[a] Division of CJD Science and Technology, Department of Prion Research, Tohoku University Graduate School of Medicine, 2-1 Seiryo-machi, Aoba-ku, Sendai 980-8575, Japan
[b] Department of Neurology and Neurological Science, Graduate School, Tokyo Medical and Dental University, Tokyo 113-8519, Japan

ARTICLE INFO

Article history:
Received 15 December 2009
Available online 29 December 2009

Keywords:
Prion protein
Mutation
Glycosylphosphatidylinositol anchor
Conversion
ω Site

ABSTRACT

Prion protein (PrP) is a glycosylphosphatidylinositol (GPI)-anchored protein, and the C-terminal GPI anchor signal sequence (GPI-SS) of PrP is cleaved before GPI anchoring. However, mutations near the GPI anchor attachment site (the ω site) in the GPI-SS have been recognized in human genetic prion diseases. Moreover, the ω site of PrP has not been identified except hamster, though it is known that amino acid restrictions are very severe at the ω and ω + 2 sites in other GPI-anchored proteins. To investigate the effect of mutations near the ω site of PrP on the conversion and the GPI anchoring, and to discover the ω site of murine PrP, we systematically created mutant murine PrP with all possible single amino acid substitutions at every amino acid residue from codon 228 to 240. We transfected them into scrapie-infected mouse neuroblastoma cells and examined the conversion efficiencies and the GPI anchoring of each mutant PrP. Mutations near the ω site altered the conversion efficiencies and the GPI anchoring efficiencies. Especially, amino acid restrictions for the conversion and the GPI anchoring were severe at codons 230 and 232 in murine PrP, though they were less severe than in other GPI-anchored proteins. Only the mutant PrPs presented on a cell surface via a GPI anchor were conversion competent. The present study shows that mutations in the GPI-SS can affect the GPI anchoring and the conversion efficiency of PrP. We clarified for the first time the ω site of murine PrP and the amino acid conditions near the ω site for the conversion as well as GPI anchoring.

© 2009 Elsevier Inc. All rights reserved.

Introduction

Prion diseases are infectious fatal neurodegenerative diseases that include scrapie in sheep and goat, bovine spongiform encephalopathy in cattle and Creutzfeldt–Jakob disease (CJD) in human, which are caused by infectious abnormal prion protein (PrP^{Sc}) that is converted from the normal cellular prion protein (PrP^{C}) [1].

PrP^{C} is attached to a cell surface via a glycosylphosphatidylinositol (GPI) anchor [2]. Shortly after the precursor PrP is fully translocated into the ER lumen, a GPI anchor is added rapidly to the acceptor amino acid, termed the ω site [3], following the cleavage of the C-terminal GPI anchor signal sequence (GPI-SS) by the action of a GPI transamidase [4].

More than 30 causative mutations in human genetic prion diseases have been recognized so far [5]. Among them, the amino acid substitutions of M232R [6–8] and M232T [9] have been reported as mutations in the GPI-SS. However, the GPI-SS is not included in the mature PrP as a consequence of a posttranslational modification, which raises a question about the effect of the mutation in the GPI-SS on the conversion of PrP.

Meanwhile, a database analysis revealed that the GPI-SS of GPI-anchored proteins has several general features but does not contain any consensus sequence [10]. In addition, the ω site of PrP has been identified only in hamster [11], of which the amino acid residues near the ω site are somewhat different from those of mouse. Therefore, the ω site of murine PrP has been only assumed to be codon 230 [4] or 231 [12] but not determined accurately, and the amino acid conditions of the GPI-SS for GPI anchoring need to be examined thoroughly.

In the present study, to investigate the effects of a single amino acid substitution near the ω site of PrP on the conversion and the GPI anchoring, we systematically examined the conversion efficiency and the GPI anchor attachment of mutant murine PrP with all possible single amino acid substitutions at every amino acid residue from codon 228 to 240 in scrapie-infected mouse neuroblastoma (ScN2a) cells. We revealed the amino acid conditions in the GPI-SS of PrP necessary for the conversion and the GPI anchor attachment and identified the ω site of murine PrP.

Materials and methods

Cell culture. ScN2a cells were kindly provided by Dr. Stanley B. Prusiner [13] and maintained in Dulbecco's modified Eagle's med-

* Corresponding author. Fax: +81 22 717 8148.
E-mail address: kitamoto@mail.tains.tohoku.ac.jp (T. Kitamoto).

0006-291X/$ - see front matter © 2009 Elsevier Inc. All rights reserved.
doi:10.1016/j.bbrc.2009.12.128

ium (Invitrogen) containing 10% fetal bovine serum (Invitrogen), 100 U/ml penicillin and 100 μg/ml streptomycin (Invitrogen) at 37 °C in 5% CO_2.

Plasmid construction. The open reading frame of mouse PrP gene was cloned into plasmid pBluescript (Stratagene) as described [14]. The epitope for the monoclonal antibody 3F4 (L108M and V111M) [15] and 19 kinds of single amino acid substitutions at every amino acid residue from codon 228 to 240 were introduced into mouse PrP gene by site-directed PCR mutagenesis as described [14]. These 3F4 epitope-tagged mutant PrP fragments were cloned into the expression vector pSPOX [16]. All amino acid numbers refer to mouse PrP sequence.

Transfection and harvest. ScN2a cells were transiently transfected with plasmid constructs using the FuGENE® 6 transfection reagent according to the manufacturer's directions (Roche Diagnostics). The medium was exchanged after 24 h of transfection. After 48 h of transfection, the cells were harvested with 1 ml of lysis buffer (10 mM Tris–HCl pH 7.5, 100 mM NaCl, 1 mM EDTA, 0.5% Triton X-100, and 0.5% sodium deoxycholate) and the cell debris and nuclei were removed by low-speed centrifugation.

Deglycosylation treatment. For the detection of the total cell-associated PrP (PrP^{total}), 20 μl of the cell lysates were boiled with the addition of 5 μl of 5 × sample buffer (10% SDS, 300 mM Tris–HCl pH 6.8, 25% 2-mercaptoethanol, 25% glycerol, and 0.05% bromophenol blue), and digested with 300 U of PNGase F (New England Biolabs) at 37 °C for 2 h. For the evaluation of the sensitivity to Endoglycosidase H treatment, 20 μl of the cell lysates were boiled with the addition of 5 μl of 5 × sample buffer and digested with 500 U of Endoglycosidase H (New England Biolabs) at 37 °C for 2 h.

Protease treatment. For the detection of the proteinase K (PK) resistant form of PrP (PrP^{res}), 480 μl of the cell lysates were digested with 20 μg/ml PK at 37 °C for 30 min in the presence of 2% sarkosyl. The digestion was terminated by adding 2 mM of Pefabloc SC (Roche Diagnostics). The digested samples were ultracentrifuged at 100,000g, 20 °C for 1 h, and the pellets were resuspended with 40 μl of sample buffer and boiled.

Phosphatidylinositol-phospholipase C (PI-PLC) treatment. Subconfluent ScN2a cells in 6-well plates were transiently transfected with plasmid constructs as described above. The medium was exchanged after 24 h of transfection. After 45 h of transfection, the medium was removed, and 1 ml of PBS containing 0.25 U of PI-PLC (Sigma–Aldrich Inc.) was added for the detection of the PrP released from the cell membrane. The cells were incubated with PI-PLC at 37 °C for 3 h before the culture supernatants were harvested. For a negative control, the cells were incubated with 1 ml of PBS. Detached cells, if any, were removed by low-speed centrifugation. For the detection of the released PrP, 40 μl of the supernatants were digested with PNGase F for the deglycosylation as described above.

Triton X-114 phase-partitioning. ScN2a cells in 10-cm dishes were washed with PBS and harvested with 1 ml of Triton X-114 lysis buffer (10 mM Tris–HCl pH 7.5, 100 mM NaCl, 1 mM EDTA, and 2% Triton X-114). These cell lysates were incubated at 4 °C for 10 min and centrifuged at 1500g, 4 °C for 5 min to pellet cell debris and nuclei. For the Triton X-114 phase-partitioning, 400 μl of the supernatants were incubated at 37 °C for 10 min and centrifuged at 9000g, 37 °C for 10 min. The upper aqueous phases were mixed with equal volume (360 μl) of Triton X-114 lysis buffer, and boiled with the addition of 180 μl of 5 × sample buffer. The lower Triton X-114 phases were mixed with 360 μl of TNE buffer (10 mM Tris–HCl pH 7.5, 100 mM NaCl, 1 mM EDTA) and incubated at 4 °C for 5 min. The phase-partitioning step was repeated two times to wash the detergent phases thoroughly. The Triton X-114 phases were mixed with 680 μl of TNE buffer, and boiled with the addition of 180 μl of 5 × sample buffer. The boiled samples were digested with PNGase F for the deglycosylation as described above.

Western blot analysis. The samples were applied to 13% SDS–PAGE and Western blotting using monoclonal antibody 3F4 (Signet Laboratories) as described [14,17]. To calculate the relative conversion efficiency of mutant PrP, the relative expression level of PrP^{res} was divided by that of PrP^{total}. All experiments were repeated independently at least three times, and representative data are shown.

Results

Single amino acid substitutions near the ω site of PrP alter the conversion efficiency, and the amino acid restrictions for the conversion are very severe at codons 230 and 232.

We first addressed the question of whether single amino acid substitutions near the ω site of PrP gene might alter the conversion efficiency. We created mutant murine PrP constructs with all possible single amino acid substitutions at every amino acid residue from codon 228 to 240 and transfected them into ScN2a cells. By the Western blot analysis, we observed the following: (i) at codons 228 and 229, each expression level of the mutant PrP^{total} was almost equal to that of WT PrP^{total} (Fig. 1A and C, gray bars; Supplementary Fig. 1A and C, gray bars), whereas the conversion efficiencies of mutant PrP substituted with C, D, E, F, W or Y at codon 228, or with D, E, F or W at codon 229 were decreased to 0.2 or less compared to that of WT PrP (Fig. 1B and D, black bars; Supplementary Fig. 1B and D, black bars); (ii) at codon 230, the relative conversion efficiencies of each PrP substituted with C, E, F, H, I, K, L, M, Q, R, W or Y were reduced to 0.2 or less (Fig. 1H and J, black bars), of which the expression levels of PrP^{total} were also relatively decreased (Fig. 1G and I, gray bars). In contrast, the relative conversion efficiencies of each PrP substituted with A, D, G, N, P, T or V were generally sustained (Fig. 1H and J, white bars), and the expression levels of PrP^{total} were also relatively maintained (Fig. 1G and I, gray bars); (iii) at codon 231, the relative expression levels of the mutant PrP^{total} only modestly varied (Fig. 1K and M, gray bars), while the relative conversion efficiency of the mutant PrP was decreased to 0.2 or less only in S231W (Fig. 1L and N, black bar); (iv) at codon 232, the relative conversion efficiencies of each PrP substituted with F, I, L, M, P, W or Y were reduced to 0.2 or less (Fig. 1R and T, black bars), and the expression levels of PrP^{total} were also relatively decreased (Fig. 1Q and S, gray bars). In contrast, the relative conversion efficiencies of each PrP substituted with A, C, D, E, G, H, K, N, Q, R, T or V were generally sustained (Fig. 1R and T, white bars), and the expression levels of PrP^{total} were also relatively maintained (Fig. 1Q and S, gray bars); (v) at every residue from codon 233 to 240, single amino acid substitutions hardly affected the conversion efficiencies of the mutant PrP or the expression levels of the mutant PrP^{total} (Supplementary Fig. 1E–j). Taken

Fig. 1. Single amino acid substitutions near the ω site of PrP can alter the conversion efficiency, and the amino acid restrictions for the conversion are very severe at codons 230 and 232 in murine PrP. (A, G, K, Q) Western blot analysis for the PrP^{total} of WT and mutations at codon 228, 230, 231 or 232, respectively, after deglycosylation with PNGase F. (B, H, L, R) Western blot analysis for the PrP^{res} of WT and mutations at codon 228, 230, 231 or 232, respectively. (C, I, M, S) The relative expression levels of mutant PrP^{total} (gray bars) and those of mutant PrP^{res} (black bars) at codon 228, 230, 231 or 232, respectively. (D, J, N, T) The relative conversion efficiencies at codon 228, 230, 231 or 232, respectively. Black bars indicate the relative conversion efficiencies reduced to 0.2 or less. (E, O) Western blot analysis for the PrP^{total} of WT and mutations at codon 230 or 232, respectively, without deglycosylation. (F, P) Western blot analysis for the PrP^{total} of WT and mutations at codon 230 or 232, respectively, after deglycosylation with Endoglycosidase H. In A, B, E–H, K, L, and O–R, molecular size markers are indicated as bars on the left side of the panels and represent 32.5, 25 and 16.5 kDa. In C, D, I, J, M, N, S and T, data represent mean ± standard deviation of three independent experiments.

together, the single amino acid substitutions near the ω site in the GPI-SS of murine PrP altered the relative expression levels as well as the relative conversion efficiencies. The amino acid restrictions for the conversion were very severe at codons 230 and 232.

The amino acid substitutions at codon 230 or 232 of PrP markedly affected the expression levels of PrP^{total} and the conversion efficiencies. Therefore, we next examined the sensitivity of N-linked glycans on each mutant PrP to Endoglycosidase H treat-

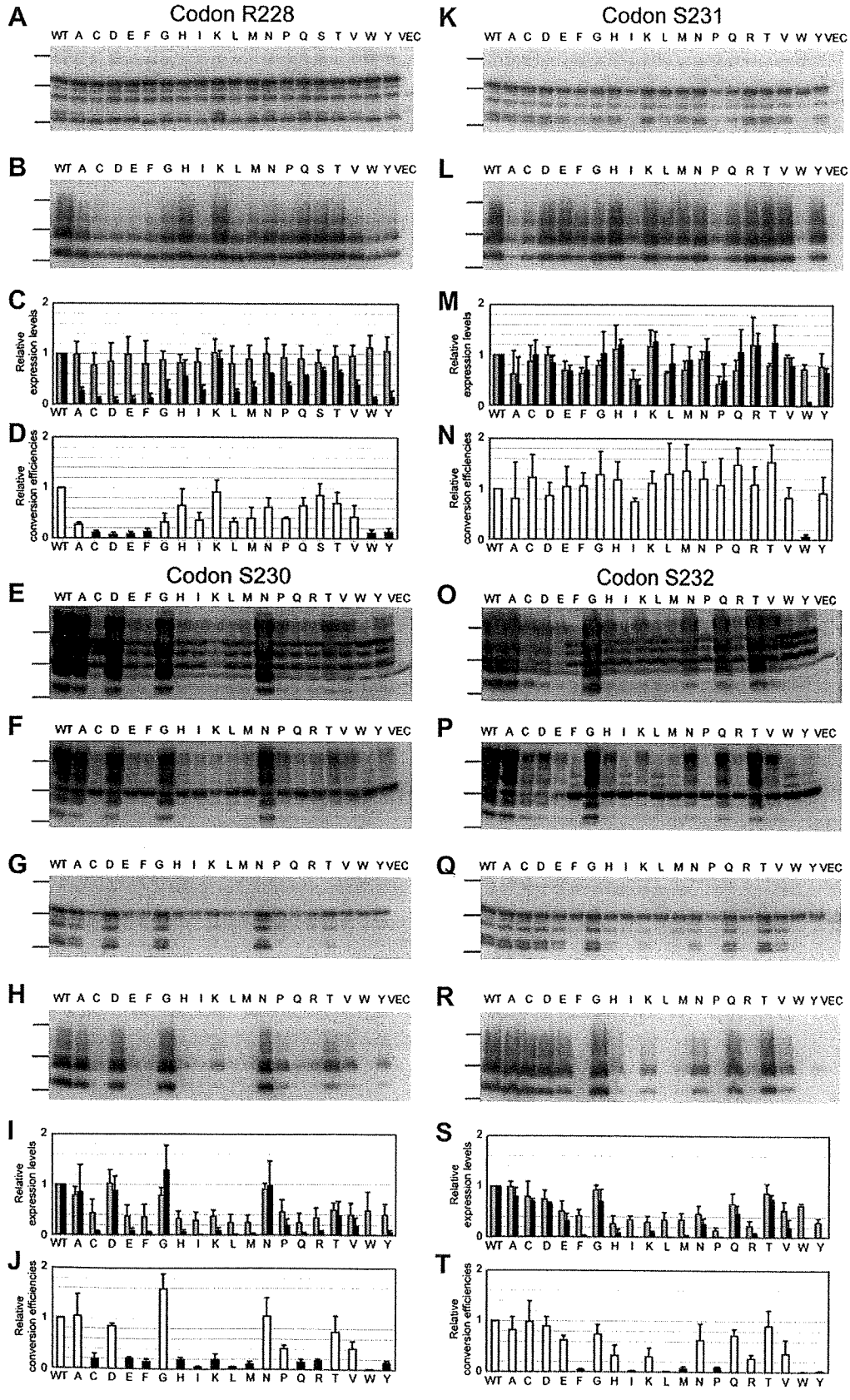

ment. If mutant PrP is misfolded and retained in the ER, the N-linked glycans on the mutant PrP should be the high mannose-type and cleaved by Endoglycosidase H. At codon 230, only the N-linked glycans of mutant PrP substituted with A, D, G, N or T were resistant to Endoglycosidase H treatment (Fig. 1E and F). At codon 232, the N-linked glycans of mutant PrP substituted with A, C, D, G, N, Q, T or V were resistant to Endoglycosidase H (Fig. 1O and P). These results suggest that the amino acid substitutions at codon 230 or 232 can cause the retention of mutant PrP in the ER and result in decreased expression levels of PrP^{total}.

Only GPI-anchored mutant PrP can be converted into PrP^{res}

The severe restrictions for the conversion at codons 230 and 232 raised the possibility that codon 230 was the ω site and codon 232 was the ω + 2 site in murine PrP. To address this possibility, we next analyzed the GPI anchoring of the mutant PrP by PI-PLC treatment. If mutant PrP is attached to a cell membrane via a GPI anchor, PI-PLC treatment of the cells results in release of the membrane-anchored PrP into the medium. The Western blot analysis of the incubation medium revealed the following: (i) at codon 228, PI-PLC cleaved all the mutant PrP as well as WT PrP (Fig. 2A); (ii) at codon 230, PI-PLC cleaved the mutant PrP substituted with A, D, G, N, P, T or V (Fig. 2B); (iii) at codon 232, PI-PLC cleaved the mutant PrP substituted with A, C, D, E, G, H, K, N, Q, R, T or V (Fig. 2C).

Since the N-linked glycans of most mutant PrPs with amino acid substitutions at codon 230 or 232 were sensitive to Endoglycosidase H treatment (Fig. 1F and P), there remained the possibility that the mutant PrPs were just misfolded and retained in the ER and could not be released by PI-PLC even if they were GPI-anchored. To address this possibility, we next performed Triton X-114 phase-partitioning to isolate GPI-anchored PrP. If mutant PrPs

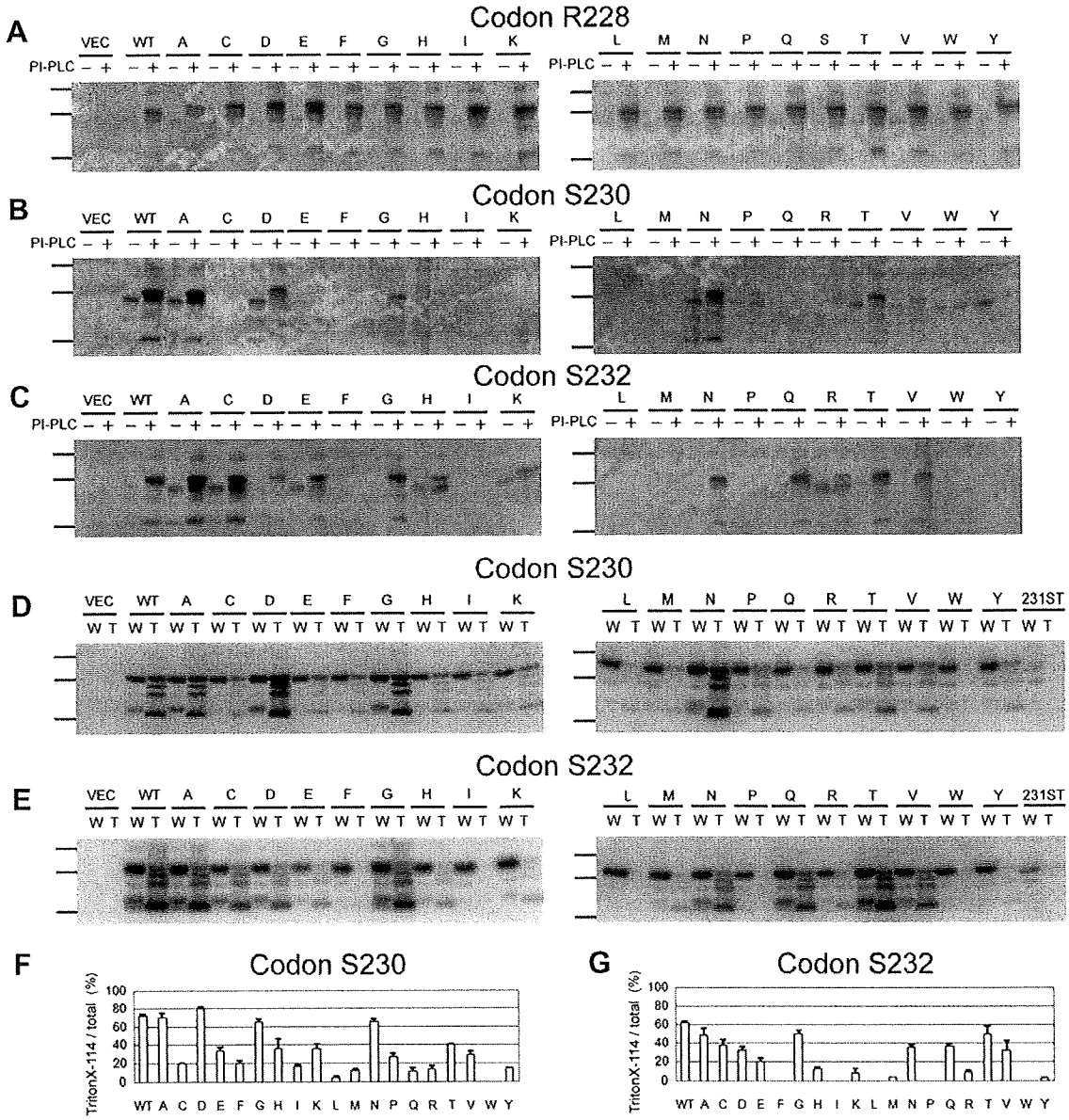

Fig. 2. Single amino acid substitutions near the ω site of PrP can alter the GPI anchoring efficiency, and the amino acid conditions for the anchoring are very tight at codons 230 and 232 in murine PrP. (A–C) The bands of released PrP were detected in WT and some mutations at codon 228, 230 or 232, respectively. Results are representative of several experiments repeated independently. (D, E) Triton X-114 phase-partitioning to isolate GPI-anchored PrP. W: water phase. T: Triton X-114 phase. 231ST: GPI-anchorless PrP with a stop codon after codon 231. (F, G) The proportion of GPI-anchored PrP in Triton X-114 phase-partitioning. Data represent mean ± standard deviation of three independent experiments. In A–E, molecular size markers are indicated as bars on the left side of the panels and represent 32.5, 25 and 16.5 kDa.

Table 1
Results are those of the comparison studies on the PrP conversion efficiencies/the released PrP with PI-PLC, respectively.

Substituting amino acids	Substituted position number of codons		
	228	230	232
W	−/+	−/−	−/−
Y	−/+	−/−	−/−
R	WT	−/−	+/+
F	−/+	−/−	−/−
H	+/+	−/−	+/+
M	+/+	−/−	−/−
E	−/+	−/−	+/+
K	+/+	−/−	+/+
Q	+/+	−/−	+/+
D	−/+	+/+	+/+
N	+/+	+/+	+/+
I	+/+	−/−	−/−
L	+/+	−/−	−/−
C	−/+	−/−	+/+
T	+/+	+/+	+/+
V	+/+	+/+	+/+
P	+/+	+/+	−/−
S	+/+	WT	WT
A	+/+	+/+	+/+
G	+/+	+/+	+/+

− means that the relative conversion efficiency of the mutant PrP was decreased to 0.2 or less, or that the mutant PrP was not released into the culture medium after PI-PLC treatment, respectively. + means that the relative conversion efficiency of the mutant PrP was sustained above 0.2 or that the mutant PrP was released into the culture medium after PI-PLC treatment, respectively.

are GPI-anchored, they should be collected within the Triton X-114 phase. At codon 230, only the mutant PrP substituted with A, D, G or N showed a relatively sustained Triton X-114/total PrP ratio compared to that of WT PrP (Fig. 2D and F). At codon 232, only the mutant PrP substituted with A, C, G, N, Q, T or V showed a relatively sustained Triton X-114/total PrP ratio (Fig. 2E and G). Therefore, we confirmed that the amino acid substitutions at codon 230 or 232 of murine PrP affected the GPI anchoring efficiencies.

Taken together, the single amino acid substitutions near the ω site of PrP altered the GPI anchoring efficiencies, and the amino acid conditions for the GPI anchoring were very tight at codons 230 and 232 in murine PrP. Furthermore, only the GPI-anchored mutant PrPs acquired resistance to the deglycosylation with Endoglycosidase H and could be converted into PrP^{res} (Table 1).

Discussion

Our study revealed three findings. First, the mutations near the ω site of PrP can alter not only the GPI anchoring efficiency but also the conversion efficiency. Second, amino acid conditions in the GPI-SS of murine PrP are very severe at codons 230 and 232 for the conversion as well as for the GPI anchoring. Finally, among mutant PrPs with amino acid substitutions in the GPI-SS, only the mutant PrPs presented on a cell surface via a GPI anchor are conversion competent. These results suggest that the loss of GPI anchoring might cause misfolding and ER-retention of the mutant PrP and result in the decreased expression level and the altered conversion efficiency.

The finding that amino acid restrictions for the GPI anchoring were very severe at codons 230 and 232 indicates that codons 230 and 232 are the ω and ω + 2 sites, respectively. A database analysis documented that the GPI-SS does not contain any consensus sequence but has several general features as follows [10]: (i) a stretch of ~10 polar amino acids (ω − 10 to ω − 1) that form a flexible linker region; (ii) amino acids of the ω site are those with small side-chains, such as G, A, S, N, D and C; (iii) the ω + 2 amino acids, the most restrictive position, are also those with small side-chains, such as G, A and S; (iv) a hydrophilic spacer region of moderately polar amino acids (ω + 3 to ω + 9 or more); and (v) a C-terminal hydrophobic sequence is variable in length but capable of spanning the membrane [3,18]. However, mutational studies with all possible single amino acid substitutions in the GPI-SS of GPI-anchored proteins have not been performed to date. Therefore, the amino acid conditions in the GPI-SS of PrP, especially near the ω site, for the GPI anchoring as well as for the conversion have not been examined completely. Our study revealed novel findings in the GPI-SS of PrP as follows: (i) at the ω site (codon 230), the amino acids essential for the GPI anchoring are not only G, A, S, N and D but also P, T and V (D or smaller amino acids except I, L and C); (ii) at the ω + 2 site (codon 232), they are C, D, E, H, K, N, Q, R, T and V as well as G, A and S (R or smaller amino acids excluding I, L, M, P and F). Taken together, these results suggest that the amino acid conditions at the ω and ω + 2 sites for the GPI anchoring are less severe in PrP than in other GPI-anchored proteins, though the amino acids at the ω site of PrP are more limited than those at the ω + 2 site (Table 1).

Amino acid substitutions in GPI-SS can alter GPI anchor attachment, and the mutant protein can be secreted into the culture medium [19] or retained in the ER [20]. Mutant PrP without the GPI anchor are secreted into the medium [21–23], while uncleaved GPI-SS causes retention of the PrP in the ER [24]. In addition, misfolded ER proteins can be degraded via a pathway termed ER-associated protein degradation [25], and a co-translocational or preemptive quality control pathway exists to reduce the burden of misfolded substrates entering the ER [26]. Since the mutant PrPs lacking GPI anchor were retained in the ER in this study, these mutant PrPs might be misfolded and degraded inside the ScN2a cells. Therefore, mutant PrPs lacking GPI anchor showed the decreased expression levels and the altered conversion efficiencies in the present study. Our finding that only the mutant PrPs presented on a cell surface via a GPI anchor are conversion competent indicates that PrP is converted after reaching the cell surface in ScN2a cells. Meanwhile, some mutant PrPs substituted at codon 228 or 229 showed decreased relative conversion efficiencies though they were GPI-anchored. At codons 228 and 229, substitutions with amino acids with negative or large side-chains might prevent the conversion of PrP independently of GPI anchoring as mutations in the core region of PrP reduced the conversion efficiency [14].

About 30 cases of genetic CJD with M232R have been reported so far [6–8], which accounts for about 13% of the genetic CJD patients in Japan. Therefore, the mutation is considered to be a causative mutation. Although the codon in murine PrP corresponding to codon 232 in human PrP has not been identified, no mutation near the ω site of murine PrP increased the conversion efficiency. Plausible explanations are as follows: (i) the amino acid sequence, especially near the ω site, is different among species; (ii) we examined the seed-dependent conversion in ScN2a cells but not the spontaneous conversion leading to the pathogenesis of genetic CJD. Although the GPI anchoring of human PrP with M232R has not been investigated sufficiently, a subpopulation of the mutant PrP could be GPI-anchorless and misfolded in the ER. The accumulation of these misfolded GPI-anchorless mutant PrP might lead to the spontaneous conversion. We need to further investigate the pathogenesis in animal models expressing human PrP with M232R and so on.

In conclusion, the present study shows that single amino acid substitutions near the ω site of PrP affect the GPI anchoring and the conversion efficiency. We clarified for the first time the ω site of murine PrP and the amino acid conditions near the ω site for the conversion as well as for the GPI anchoring.

Acknowledgments

We thank H. Suda for technical assistance, K. Teruya for critical advice and B. Bell for critical review of the manuscript. This study

was supported by the Promotion of Fundamental Studies in Health Science of National Institute of Biomedical Innovation (T.K.), a grant from the Ministry of Health, Labor and Welfare (A.K. and T.K.), a Grant-in-Aid for Scientific Research from the Ministry of Education, Culture, Sports, Science and Technology (A.K. and T.K.), and Grants-in-Aid from the Research Committee of Prion disease and Slow Virus Infection, the Ministry of Health, Labor and Welfare of Japan (A.K. and H.M.).

Appendix A. Supplementary data

Supplementary data associated with this article can be found, in the online version, at doi:10.1016/j.bbrc.2009.12.128.

References

[1] S.B. Prusiner, Prions, Proc. Natl. Acad. Sci. USA 95 (1998) 13363–13383.
[2] N. Stahl, D.R. Borchelt, K. Hsiao, S.B. Prusiner, Scrapie prion protein contains a phosphatidylinositol glycolipid, Cell 51 (1987) 229–240.
[3] P. Orlean, A.K. Menon, GPI anchoring of protein in yeast and mammalian cells, or: how we learned to stop worrying and love glycophospholipids, J. Lipid Res. 48 (2007) 993–1011.
[4] J. Tatzelt, K.F. Winklhofer, Folding and misfolding of the prion protein in the secretory pathway, Amyloid 11 (2004) 162–172.
[5] S. Mead, Prion disease genetics, Eur. J. Hum. Genet. 14 (2006) 273–281.
[6] T. Kitamoto, M. Ohta, K. Doh-ura, et al., Novel missense variants of prion protein in Creutzfeldt–Jakob disease or Gerstmann–Sträussler syndrome, Biochem. Biophys. Res. Commun. 191 (1993) 709–714.
[7] Y. Shiga, K. Satoh, T. Kitamoto, et al., Two different clinical phenotypes of Creutzfeldt–Jakob disease with a M232R substitution, J. Neurol. 254 (2007) 1509–1517.
[8] L. Zheng, J. Longfei, Y. Jing, et al., PRNP mutations in a series of apparently sporadic neurodegenerative dementias in China, Am. J. Med. Genet. B 147B (2008) 938–944.
[9] J. Bratosiewicz, P.P. Liberski, J. Kulczycki, R. Kordek, Codon 129 polymorphism of the PRNP gene in normal Polish population and in Creutzfeldt–Jakob disease, and the search for new mutations in PRNP gene, Acta Neurobiol. Exp. (Wars) 61 (2001) 151–156.
[10] B. Eisenhaber, P. Bork, F. Eisenhaber, Sequence properties of GPI-anchored proteins near the omega-site: constraints for the polypeptide binding site of the putative transamidase, Protein Eng. 11 (1998) 1155–1161.
[11] N. Stahl, M.A. Baldwin, A.L. Burlingame, S.B. Prusiner, Identification of glycoinositol phospholipid linked and truncated forms of the scrapie prion protein, Biochemistry 29 (1990) 8879–8884.
[12] D.R. Taylor, N.M. Hooper, The prion protein and lipid rafts, Mol. Membr. Biol. 23 (2006) 89–99.
[13] D.A. Butler, M.R. Scott, J.M. Bockman, et al., Scrapie-infected murine neuroblastoma cells produce protease-resistant prion proteins, J. Virol. 62 (1988) 1558–1564.
[14] S. Ikeda, A. Kobayashi, T. Kitamoto, Thr but Asn of the N-glycosylation sites of PrP is indispensable for its misfolding, Biochem. Biophys. Res. Commun. 369 (2008) 1195–1198.
[15] R.J. Kascsak, R. Rubenstein, P.A. Merz, et al., Mouse polyclonal and monoclonal antibody to scrapie-associated fibril proteins, J. Virol. 61 (1987) 3688–3693.
[16] M.R. Scott, R. Köhler, D. Foster, S.B. Prusiner, Chimeric prion protein expression in cultured cells and transgenic mice, Protein Sci. 1 (1992) 986–997.
[17] M. Asano, S. Mohri, J.W. Ironside, et al., vCJD prion acquires altered virulence through trans-species infection, Biochem. Biophys. Res. Commun. 342 (2006) 293–299.
[18] T. Kinoshita, M. Fujita, Y. Maeda, Biosynthesis, remodelling and functions of mammalian GPI-anchored proteins: recent progress, J. Biochem. 144 (2008) 287–294.
[19] M.E. Lowe, Site-specific mutations in the COOH-terminus of placental alkaline phosphatase: a single amino acid change converts a phosphatidylinositol-glycan-anchored protein to a secreted protein, J. Cell Biol. 116 (1992) 799–807.
[20] R. Micanovic, L.D. Gerber, J. Berger, K. Kodukula, S. Udenfriend, Selectivity of the cleavage/attachment site of phosphatidylinositol-glycan-anchored membrane proteins determined by site-specific mutagenesis at Asp-484 of placental alkaline phosphatase, Proc. Natl. Acad. Sci. USA 87 (1990) 157–161.
[21] K.F. Winklhofer, J. Heske, U. Heller, et al., Determinants of the in vivo folding of the prion protein. A bipartite function of helix 1 in folding and aggregation, J. Biol. Chem. 278 (2003) 14961–14970.
[22] B. Chesebro, M. Trifilo, R. Race, et al., Anchorless prion protein results in infectious amyloid disease without clinical scrapie, Science 308 (2005) 1435–1439.
[23] S. Kiachopoulos, A. Bracher, K.F. Winklhofer, J. Tatzelt, Pathogenic mutations located in the hydrophobic core of the prion protein interfere with folding and attachment of the glycosylphosphatidylinositol anchor, J. Biol. Chem. 280 (2005) 9320–9329.
[24] M.C. Field, P. Moran, W. Li, G.A. Keller, I.W. Caras, Retention and degradation of proteins containing an uncleaved glycosylphosphatidylinositol signal, J. Biol. Chem. 269 (1994) 10830–10837.
[25] K. Nakatsukasa, J.L. Brodsky, The recognition and retrotranslocation of misfolded proteins from the endoplasmic reticulum, Traffic 9 (2008) 861–870.
[26] S.W. Kang, N.S. Rane, S.J. Kim, et al., Substrate-specific translocational attenuation during ER stress defines a pre-emptive quality control pathway, Cell 127 (2006) 999–1013.

ADVERTISEMENT
Search over 3 million articles on WILEY InterScience
Journals | Online Books | Reference Works | Databases

Systems Maintenance, Monday, 18 January 2010
My Cart | My Profile | Log In | Athens Log In

WILEY InterScience®
DISCOVER SOMETHING GREAT

Microbiology and Immunology

Microbiology and Immunology

Published Online: 20 Nov 2009

© 2010 Japanese Society for Bacteriology, Japanese Society for Virology, Japanese Society for Host Defense Research, and Blackwell Publishing Asia Pty Ltd

Get Sample Copy
Recommend to Your Librarian
Save journal to My Profile
Set E-Mail Alert
Email this page
Print this page
RSS web feed (What is RSS?)

Save Article to My Profile | Download Citation | Request Permissions
< Previous Abstract | Next Abstract >

Abstract | Full Text: PDF (Size: 540K) | Related Articles | Citation Tracking

A novel anti-prion protein monoclonal antibody and its single-chain fragment variable derivative with ability to inhibit abnormal prion protein accumulation in cultured cells

Yoshihisa Shimizu [1], Yuko Kaku-Ushiki [2], Yoshifumi Iwamaru [1], Tamaki Muramoto [3], Tetsuyuki Kitamoto [3], Takashi Yokoyama [1], Shirou Mohri [1] and Yuichi Tagawa [4]

[1] Prion Disease Research Center, National Institute of Animal Health, 3-1-5 Kannondai, Tsukuba, Ibaraki 305-0856, Japan, [2] Nippi Research Institute of Biomatrix, 520-11 Kuwabara, Toride, Ibaraki 302-0017, Japan, [3] Department of Prion Research, Tohoku University Graduate School of Medicine, 2-1 Seiryou-machi, Aoba-ku, Sendai, Miyagi 980-8575, Japan, [4] National Institute of Animal Health, 3-1-5 Kannonndai Tsukuba, Ibaraki 305-0856, Japan

Correspondence
Yuichi Tagawa, National Institute of Animal Health, 3-1-5 Kannondai, Tsukuba, Ibaraki 305-0856, Japan. Tel.: 81-29-838-7743; fax: 81-29-838-7740; email: ytagawa@affrc.go.jp

KEYWORDS
anti-prion effect • monoclonal antibody • single-chain fragment variable region

ABSTRACT

Monoclonal antibodies (mAbs) T1 and T2 were established by immunizing prion protein (PrP) gene ablated mice with recombinant mouse PrP (MoPrP) of residues 121–231. Both mAbs were cross-reactive with PrP from hamster, sheep, cattle and deer. A linear epitope of mAb T1 was identified at residues 137–143 of MoPrP and buried in cellular PrP (PrP^C) expressed on the cell surface. mAb T1 showed no inhibitory effect on accumulation of scrapie isoform of PrP (PrP^{Sc}) in cultured scrapie-infected neuroblastoma (ScN2a) cells. In contrast, mAb T2 recognized a discontinuous epitope ranged on or structured by residues 132–217 and this epitope was exposed on the cell surface PrP^C. mAb T2 showed an excellent inhibitory effect on PrP^{Sc} accumulation in vitro at a 50% inhibitory concentration of 0.02 μg/ml (0.14 nM). Single-chain fragment variable (scFv) form of mAb T2 (scFv T2) was secreted in neuroblastoma (N2a58) cell cultures by transfection through eukaryotic secretion vector. Coculturing of ScN2a cells with scFv T2-producing N2a58 cells induced a clear inhibition effect on PrP^{Sc} accumulation, suggesting that scFv T2 could be potentially an immunotherapeutic tool for prion diseases by inhibition of PrP^{Sc} accumulation.

Received 25 August 2009; revsied 8 October 2009; accepted 22 October 2009

DIGITAL OBJECT IDENTIFIER (DOI)

10.1111/j.1348-0421.2009.00190.x About DOI

Related Articles

Microbiology and Immunology

Microbiol Immunol 2009; **53**: 704–707
doi:10.1111/j.1348-0421.2009.00169.x

NOTE

Intraspecies transmission of L-type-like bovine spongiform encephalopathy detected in Japan

Shigeo Fukuda[1*], Yoshifumi Iwamaru[2*], Morikazu Imamura[2], Kentarou Masujin[2], Yoshihisa Shimizu[2], Yuichi Matsuura[2], Yujing Shu[2], Megumi Kurachi[2], Kazuo Kasai[2], Yuichi Murayama[2], Sadao Onoe[1], Ken'ichi Hagiwara[3], Tetsutaro Sata[4], Shirou Mohri[2], Takashi Yokoyama[2] and Hiroyuki Okada[2]

[1]Molecular Biotechnology Laboratory, Hokkaido Animal Research Center, Shintoku, Hokkaido 081-0038, Japan [2]Prion Disease Research Center, National Institute of Animal Health, 3-1-5 Kan-nondai, Tsukuba, Ibaraki 305-0856, Japan [3]Departments of Biochemistry and Cell Biology, and [4]Pathology, National Institute of Infectious Diseases, Toyama 1-23-1 Shinjuku-ku, Tokyo, 162-8640, Japan

ABSTRACT

It has been assumed that the agent causing BSE in cattle is a uniform strain (classical BSE); however, different neuropathological and molecular phenotypes of BSE (atypical BSE) have been recently reported. We demonstrated the successful transmission of L-type-like atypical BSE detected in Japan (BSE/JP24 isolate) to cattle. Based on the incubation period, neuropathological hallmarks, and molecular properties of the abnormal host prion protein, the characteristics of BSE/JP24 prion were apparently distinguishable from the classical BSE prion and closely resemble those of bovine amyloidotic spongiform encephalopathy prion detected in Italy.

Key words atypical bovine spongiform encephalopathy, cattle, L-type-like, transmission.

TSE, including BSE and Creutzfeldt–Jakob disease, are neurodegenerative and fatal disorders in humans and animals. The key event in the pathogenesis of TSE is the conformational change from the normal host prion protein (PrP^{C}) to the abnormal, disease-associated form (PrP^{Sc}), which is thought to be the main, if not the only, constituent of the TSE agents. Classical BSE was first recognized in the United Kingdom (UK) in 1986 (1), and has subsequently spread to other European countries, Japan and North America. Until recently, it was believed that the BSE agent was a single strain based on biological, neuropathological and biochemical characteristics in field BSE cases (2–4). However, since 2003, different neuropathological and molecular phenotypes of BSE (atypical BSE) have been reported (5). At present, atypical BSE are classified as the H-type and L-type according to the higher and lower molecular masses of the unglycosylated form of proteinase K (PK)-treated PrP^{Sc} in western blot analysis, respectively, compared with those from classical BSE isolates (6). Among the L-type BSE cases reported from various countries (5), the Italian L-type BSE cases were further characterized by the presence of PrP-positive amyloid plaques in the brain (7) and is termed as BASE. BASE prion was experimentally transmitted to cattle, and the phenotypes of BASE prion have been characterized in detail (8). However, it remains to be determined whether the L-type BSE prions detected in other countries are identical to BASE prion and are classified into a single prion strain. Resolving this issue is crucial for future research aimed at exploring the origin of atypical BSE, assessing the risk of atypical BSE and reviewing of the current administrative measures for BSE controls.

Correspondence
Hiroyuki Okada, Prion Disease Research Center, National Institute of Animal Health, Kannonndai 3-1-5, Tsukuba, Ibaraki 305-0856, Japan. Tel & fax: +81-29-838-7757; email: okadahi@affrc.go.jp

*These authors contributed equally to this work.

Received 7 May 2009; revised 2 August 2009; accepted 4 August 2009.

List of Abbreviations: BASE, bovine amyloidotic spongiform encephalopathy; BSE, bovine spongiform encephalopathy; mAb, monoclonal antibody; PK, proteinase K; TSE, transmissible spongiform encephalopathy.

© 2009 The Societies and Blackwell Publishing Asia Pty Ltd

In Japan, two atypical BSE cases have been identified to date. The first case showed an L-type-like electrophoretic mobility of the unglycosylated PrP^{Sc} on western blot analysis (9). The second case was identified in an aged beef cattle, Japanese Black (BSE/JP24), and showed PrP-positive amyloid plaques in histopathological examination of the brain and a distinct glycoform profile (10). Although such properties seem to be similar to those reported in a BASE case (7), unlike with the BASE prion, shortening of the incubation periods was observed in bovinized mice serially passaged with the BSE/JP24 prion (11). Thus, it remains controversial whether the BSE/JP24 prion is identical to the BASE prion. These observations prompted us to characterize the phenotypes of the BSE/JP24 prion propagated in its natural host by comparison with those of the classical BSE prion. Hence, we have inoculated with brain homogenates from classical BSE and BSE/JP24 isolates into Holstein cattle and assessed their risk against cattle species.

This study was approved by the Animal Ethical Committee and the Animal Care and Use Committee of National Institute of Animal Health, and Hokkaido Animal Research Center.

Six Holstein calves aged 2–3 months were intracerebrally inoculated with 1 ml of 10% (w/v) brain homogenates prepared from the medulla oblongata of classical BSE prion-affected cattle from the UK ($n = 3$) or BSE/JP24 ($n = 3$). The cattle were clinically monitored for signs of disease. The BSE/JP24 prion-affected cattle appeared to display the clinical signs indicative of BSE, such as mild anxiety and/or hyperesthesia evoked by sudden loud noises or waving of a clipboard at 344 ± 14 (mean ± SD) days post inoculation (dpi). The time of onset of clinical signs in BSE/JP24 prion-affected cattle was substantially earlier than that in cattle inoculated with classical BSE prion in our experiments (at 548 ± 25 dpi) or than that in a previous study (12). With disease progression, both experimentally transmitted cattle showed an ataxic gait, which appeared to be due to uncoordinated hind limbs and had difficulty rising in the terminal stage of the disease. In accordance with a recent report describing the differences in clinical signs between BASE prion-affected and classical BSE prion-affected cattle (8), the BSE/JP24 prion-affected cattle were inactive and displayed little aggression.

We killed the classical BSE and BSE/JP24 prion-affected animals at the terminal stage of disease with incubation periods of 675 ± 57 and 486 ± 11 dpi, respectively (Table 1). A shorter incubation period was observed previously in transgenic mice and cattle challenged with the BASE and German L-type BSE prion (8, 13), and in transgenic mice challenged with Japanese L-type-like BSE prion (11). Thus, the short incubation period in experimental transmission might be a common feature of BASE, L-type and L-type-like BSE prion. We then examined for the accumulation of PrP^{Sc} in brain tissues by western blot and immunohistochemical analyses. Western blot analysis for PrP^{Sc} from PK-treated brain homogenates was carried out as described previously (14). To detect PK-treated PrP^{Sc}, anti-PrP mAbs 6H4 (Roche Diagnostics, Basel, Switzerland) and T2 (15) were used (Fig. 1a and b). The unglycosylated fragments of PK-treated PrP^{Sc} derived from BSE/JP24 prion-affected cattle migrated slightly faster than those from the classical BSE prion-affected cattle (Fig. 1b). The signal intensities in di- mono-, and non-glycosylated fragments of PK-treated PrP^{Sc} were measured and semiquantified by densitometric analysis (Fig. 1a and c). The relative amounts of these fragments from BSE/JP24 prion-affected cattle resembled those from the original BSE/JP24 isolate. The glycoform ratios were distinguishable from those observed in classical BSE prion-affected cattle. These data suggest that the molecular properties of PrP^{Sc} from BSE/JP24 prion were sustained in the transmitted cattle.

Vacuolar lesion profile was determined in hematoxylin–eosin-stained sections as described previously (3). For the immunohistochemical detection of PrP^{Sc}, dewaxed sections were pretreated with the chemical solutions as described previously (16) and immunolabeled with mAbs F99/97.6.1 (VMRD, Pullman, WA, USA) and T1 (17) using the tyramide signal amplification system (NEN Life Science Products, Boston, MA, USA). Vacuolation was more severe in the midbrain, thalamus, hypothalamus and frontal cortex (Fig. 2a) of BSE/JP24 prion-affected cattle compared to that of classical BSE prion-affected cattle. Immunohistochemical analysis showed that the pattern of PrP^{Sc} deposition in BSE/JP24 prion-affected cattle was characterized by diffuse synaptic-punctuate staining, low-grade stellate-type PrP^{Sc} deposits, and amyloid PrP plaques (Fig. 2b). However, no striking differences were identified in the topography of PrP^{Sc} deposition between

Table 1. Incubation period and clinical duration in BSE and BSE/JP24 prion-affected cattle

Code	Breed	Inoculum	Incubation time (days)	Clinical duration (days)
4394	Holstein	Classical BSE	610	77
4437	Holstein	Classical BSE	700	167
5087	Holstein	Classical BSE	716	139
			Mean: 675 ± 57	Mean: 128 ± 46
528	Holstein	BSE/JP24	497	160
1061	Holstein	BSE/JP24	476	113
5566	Holstein	BSE/JP24	484	151
			Mean: 486 ± 11	Mean: 141 ± 25

© 2009 The Societies and Blackwell Publishing Asia Pty Ltd